IN SITU DETERMINATION OF THE LOSS FACTORS FOR SIMPLE MULTI-MODAL STRUCTURES

by

Alain Rémont,

Ingénieur Civil Physicien A.Ir.Br.

Department of Mechanical Engineering,

University of Adelaide

Thesis submitted in accordance
with the requirements for the degree of

DOCTOR OF PHILOSOPHY

December 1982

TABLE OF CONTENTS

SUMMARY

The flow of vibrational energy between linearly coupled multi-modal resonant structures can be modelled by a set of parameters known as 'Loss Factors'. A survey of the literature on the subject shows that the loss factors have been calculated or measured for some particular cases only. Further progress on the theoretical side is impeded by the complexity of the problem and good experimental evidence is therefore highly desirable.

Previous methods for measuring the loss factors are reviewed and the 'in situ' method is examined in detail. It is noted that only the 'in situ' method yields the actual loss factors. Particular attention is given to how the energy balance equations are constructed from specific measurements. Also, the question of the accuracy of the method is studied carefully; the experimental errors are amplified by sensitivity coefficients larger than unity.

The 'in situ' method is then applied (over five octave bands) to a test structure consisting of two thin steel plates welded at right angles to each other. A digital system is designed to carry out these experiments. The sampling of data, the computations and algorithms, the hardware etc. are described extensively. A brief comparison is made with a previous (unsuccessful) attempt which used analogue techniques. Also, future improvements like dedicated hardware or more sophisticated algorithms are discussed. The loss factors obtained experimentally are then examined closely. The influence of the sensitivity coefficients is evidenced by the internal loss factors. Various theoretical predictions for the coupling loss factors are compared with the values determined 'in situ'.

It is shown how the actual loss factors of a simple multi-modal stucture can be determined experimentally by means of a digital sytem. Large amounts of data and long computing times are inevitable. Also, experimental errors are amplified by sensitivity coefficients and substantial inaccuracy can result. Excellent agreement is found with some theoretical predictions. Finally, it is suggested that the 'in situ' method is limited to structures consisting of up to four coupled multi-modal systems.

...ooo000ooo...

STATEMENT OF ORIGINALITY

It is hereby acknowledged that this thesis contains no material which has been accepted for the award of any other degree or diploma in any University, and that to the best of the author's knowledge and belief, this thesis contains no material which has been previously published or written by another person, except where due reference is made in the text.

15. 12. '82

Alain Rémont

ACKNOWLEDGEMENTS

L'auteur tient à remercier en premier lieu sa famille proche. Sans leur constant soutien, tant moral que matériel, pendant plus de quatre années de séparation, ce projet n'aurait jamais été mené à bien et encore moins entrepris !

La Société Royale Belge des Ingénieurs et des Industriels (S.R.B.I.I.), l'Association des Ingénieurs sortis de Bruxelles (A.Ir.Br.) ainsi que le Fonds Lefranc, ont également contribué à l'aboutissement de ce projet et ont droit à toute la gratitude de l'auteur. Enfin plusieurs personnalités ont assisté l'auteur de facon précieuse au début de son entreprise et il tient à leur témoigner sa profonde reconnaissance : Mr. A. Mechelynck (Président A.Ir.Br.), Mr. P. Klees (Président U.A.E.), Prof. R. van den Damme et Prof. I. de Magnée.

This research project was conducted in the Mechanical Engineering Department of the University of Adelaide, under the aegis of Prof. R.E. Luxton. The author would like to express his appreciation to Prof. Luxton and to Dr. J.M. Pickles, Chairman of the Department, for their continued support and interest throughout the project.

The author wishes to express his deep gratitude to his supervisor Dr. D.A. Bies for his outstanding help and advice. His assistance in the preparation of this thesis was also much appreciated. Special thanks are due to Mr. R. Curtin and Mr. K. Nicholle for their expert advice on computing matters. The author is also grateful to the Technical Staff for their dedicated assistance, and Ian Modistach in particular, for producing such reliable pieces of equipment.

The project was financed by a University of Adelaide Research Grant; this support is gratefully acknowledged.

Last but not least, Ms. S. Scott devoted some of her spare-time to the painstaking exercise of proof-reading the original manuscript, for which the author is much indebted to her.

...oooOOOooo...

INTRODUCTION

In practical problems dealing with a resonant structure, it is essential to be able to determine the distribution and the flow of vibrational energy between the elements of that structure. This task is well understood when only a few resonant modes play a significant role in storing, dissipating and transferring the vibrational energy. However, when many modes take an active part in the process, an exact analytical or numerical solution is rarely possible. Large or light-weight structures are typical examples of such situations, particularly when driven at high frequencies - e.g. a large ship powered by a high-speed turbine, a space vehicle made of very flimsy elements, a turbulent boundary layer around the wings of an aeroplane etc. An alternate approach to dealing with such multi-modal structures is offered by a formalism which is known as Statistical Energy Analysis.

Statistical Energy Analysis describes the flow and storage of vibrational energy between groups of similar modes by a linear system of algebraic equations. These equations express the steady-state energy balance of each group of modes, using a set of non-negative parameters called 'loss factors'. For each group of similar modes, the loss factors are defined as follows. The internal loss factor is the proportion of the average stored energy which is dissipated. The coupling loss factors are the respective proportions of the average stored energy which are transmitted to other mode groups. Thus a multi-modal structure which can be split into groups of similar modes is characterized by the loss factors of these groups.

To date, the knowledge of coupling loss factors has relied on wave-transmission type calculations or empirical formulae. The internal loss factors are usually obtained from decay-rate experiments or some-

times more simply by an 'educated guess'. To make more effective use of Statistical Energy Analysis than has been previously possible, it would be very desirable to be able to measure the loss factors on existing structures.

Theoretically, this can be done from a knowledge of injected powers and stored energies by inverting the equations of the analysis. However, previous attempts to invert the equations and use measured or estimated quantities to determine unknown internal and coupling loss factors have led to negative values for these quantities, with the exception of a two plate structure investigated by Bies and Hamid. Negative values of the loss factors are an impossibility if the energy balance equations are to be believed.

This project was aimed at overcoming the difficulties previously encountered with the in situ determination of the Statistical Energy Analysis loss factors. Three stages were thought appropriate for this purpose :- firstly, a detailed analysis of the method, its inherent drawbacks and advantages; secondly, to develop an experimental technique to implement this method on built-up structures; thirdly, to apply this technique to a simple multi-modal structure, compile the experimental results and draw general conclusions.

In this thesis, the results obtained during those three stages are described in detail.

...ooo000ooo...

REVIEW OF PREVIOUS WORK

Resonant vibrations do not always lend themselves to a deterministic analysis. Physical irregularities and uncertainties may result in a rather poor knowledge of modal quantities, or the number of modes may be so high as to render an analytical approach too cumbersome. Also, the forces acting upon the resonant system may be of a random nature, e.g. turbulent boundary layer, jet noise. Typical examples are found in room acoustics or random vibration of lightweight structures. In such cases however, a statistical approach may be applicable, whereby characteristics of groups of modes are examined rather than individual modes. This is the purpose of a formalism which has become known as Statistical Energy Analysis (SEA).

Statistical Energy Analysis aims to describe a resonant system in terms of the time-average flow of vibrational energy between groups of modes. The advantages of such an approach are firstly, that energy is readily associated with more specific dynamic variables such as strain, mean square pressure, radiated sound etc. Secondly, the SEA model of the resonant system consists simply of a set of linear equations, one for the energy balance of each mode group. These equations result from theoretical calculations of the time-average power flow between linearly coupled oscillators driven by broad-band white noise.

The first such calculation was performed by Lyon and Maidanik (Lyon and Maidanik, 1962) and established that the time-average power flow was proportional to the difference between the uncoupled time-average modal energies of two weakly coupled oscillators. The simplicity of this result was very appealing and it is probably fair to say that it was that result which initiated Statistical Energy Analysis. Next, Newland calculated the power flow between two oscillators (Newland 1966) and between two groups of oscillators (Newland 1968). In the case of weak coupling, he found the power

flow to be proportional to the difference between the average modal energies and to the average shift of natural frequencies, introduced by the coupling. The latter result readily provided a means of estimating the proportionality constant. The case of strong coupling between two oscillators was solved by Scharton and Lyon (Scharton and Lyon, 1968). They proved the time-average power flow to be proportional to the difference of the time-average actual total energies. The result held for two oscillators, and also for N identical oscillators coupled identically to each other. Unlike previous calculations, the type of coupling was the most general linear conservative coupling (i.e. stiffness, gyroscopic and inertial coupling) and was of arbitrary strength. Ungar presented an informative review of such calculations, and showed how far SEA could be applied to vibrating systems as opposed to modes or groups of modes (Ungar, 1967). An interesting point was that the normal modes of a vibrating system could form a SEA model, either if the modal energies of each group were equal, or if the couplings between the modes of 2 groups were equal. Scharton and Lyon had introduced a new way of determining the proportionality constant between power flow and energy difference, using a wave-transmission approach (Scharton and Lyon, 1968). Their result was compared with Newland's by Crandall and Lotz (Crandall and Lotz, 1971), who found agreement for weak coupling only. Statistical Energy Analysis, as applied to vibrating systems was examined by Davies in the case of coupling at discrete points (Davies,1973). He found proportionality between time-average power flow and uncoupled time-average modal energy difference. This proportionality, and various estimates of the proportionality constant were checked successfully by Lotz and Crandall for a beam to beam and a plate to plate system (Lotz and Crandall, 1973) coupled at a point by a weak spring. Similarly, Remington and Manning examined a rod-spring-rod system under longitudinal vibration

(Remington and Manning, 1975). The SEA proportionality constant they obtained by a wave-transmission calculation compared well with an exact calculation, both for weak and strong coupling. The transition from weak to strong coupling was investigated for coupled oscillators (Chandiramani, 1978) and for coupled dynamical systems (Smith, 1979).

In parallel with these calculations, experimental evidence was produced to support a statistical approach. Maidanik used a statistical method to estimate the response of ribbed panels to acoustic excitation (Maidanik, 1962). Lyon and Eichler studied the random vibration of connected structures like a beam-plate and a plate-plate system (Lyon and Eichler, 1964). Lyon and Scharton investigated the energy transmission through a plate-beam-plate system (Lyon and Scharton, 1965). The actual SEA equations were put to the test on a multipanel structure by Ungar and Koronaios (Ungar and Koronaios, 1968). Another successful example was performed by Crocker and Price in measuring the transmission loss of a panel (Crocker and Price, 1969). More recently, Swift found good agreement between predicted and measured energy ratios on multipanel structures, using a wave-transmission method to compute the SEA coefficients (Swift, 1977). Statistical Energy Analysis has also been applied fairly successfully to more general problems, e.g. ship vibrations (Ødegaard Jensen, 1976). Bies and Hamid investigated a two-plate structure (Bies and Hamid, 1980). They compared the steady-state and decay-rate approaches, and measured the SEA coefficients using an 'in situ' method.

The current state of SEA was compiled very thoroughly in a text on the subject by Lyon (Lyon, 1975). The text includes theoretical background, experimental techniques and what is surely the most exhaustive bibliography on the subject. The general conclusion of the text is that the SEA equations hold for systems of mode groups which contain similar modes, the coupling between the groups being the general, linear, conservative type and of arbitrary strength. Under these conditions,

the variables are the actual time-average total energies of the mode groups.

This result is very appealing in practice: through the SEA coefficients, which describe the loss and transfer of energy, the actual total energies of groups of similar modes are simply related by a set of linear equations. The transfer coefficients have been dealt with satisfactorily for a few particular structures as outlined above. As for the coefficients which characterize the loss of energy, they have been documented experimentally and empirically for typical structural materials (Heckl, 1962 - Beranek, 1971 - Cremer and Heckl and Ungar, 1973 - Lyon, 1975) but are liable to large uncertainties in actual built-up structures.

At present, the limitation of SEA is two-fold. Firstly, the validity of SEA has been established theoretically only for specific conditions, although the study of asymptotically correct cases has suggested a wider range of application. Unfortunately, the analytical study of multimodal systems seems to require some formidable algebra, unless some rather drastic simplifications are made.† Therefore, further knowledge of this aspect probably depends more on experimental evidence than on new theories, as Fahy pointed out (Fahy, 1974). Secondly, although particular systems have been studied successfully (see above), there is no general method to determine the SEA coefficients on existing structures. Since the accuracy of an SEA model depends on the knowledge of these coefficients, this is a serious drawback. Several standard techniques can be combined, but success depends on the particular problem at hand (Brooks and Maidanik, 1977). Moreover, these standard techniques do not always seem adequate, e.g. decay-rate experiments used to determine steady-state quantities or estimates obtained from uncoupled systems applied to coupled systems.

†See Appendix

In summary, to make more effective use of SEA than has been previously possible, it would be distinctly advantageous to be able to measure the various quantities in situ in existing structures. This would improve known models, and hopefully extend SEA techniques to more complex and practical situations.

...ooo000ooo...

THE LOSS FACTORS

2.1 The SEA Model and Equations

An SEA model consists of a series of subsystems. Each subsystem is a collection of resonant modes which play significant and almost identical roles in the flow of vibrational energy through the actual physical system. The subsystems exchange energy. They also receive energy from the outside world and dissipate some energy. If the SEA model is to be useful, one needs simple and general expressions for the average energy dissipated by a subsystem, and for the average energy flow between two subsystems.

Multimodal systems under broad-band excitation have been studied theoretically, and experiments have supported these calculations for simple resonant structures (see Chapter 1). These studies show that for each subsystem, the average energy dissipated per unit time P^{diss} is proportional to the average total stored energy E,

$$P^{diss} = \eta \, \omega_c \, E$$

where ω_c is the centre radian frequency of the frequency band containing the modes, and η is the 'Internal Loss Factor' of the subsystem over that frequency band. The same studies show that the average power transmitted between subsystems i and j is

$$P_{ij}^{trans} = \eta_{ij} \, \omega_c \, E_i - \eta_{ji} \, \omega_c \, E_j$$

where η_{ij} $(i \neq j)$ is the 'Coupling Loss Factor' between subsystems i and j over the frequency band centred at ω_c. Thus, the energy balance for subsystem i is written

$$P_i^{inj} = P_i^{diss} + \sum_{\substack{j=1 \\ (j \neq i)}}^{M} P_{ij}^{trans}$$

$$P_i^{inj} / \omega_c = \eta_{ii} E_i + \sum_{\substack{j=1 \\ (j\neq i)}}^{M} \eta_{ij} E_i - \sum_{\substack{j=1 \\ (j\neq i)}}^{M} \eta_{ji} E_j$$

P_i^{inj} is the average power injected to subsystem i, M is the number of subsystems connected to subsystem i, η_{ii} is the internal loss factor of subsystem i. Note that in general, $\eta_{ij} \neq \eta_{ji}$, rather $\eta_{ij} N_i = \eta_{ji} N_j$, where N_i and N_j are the total number of modes in subsystem i and j respectively.

These energy balance equations, one for each subsystem, establish a link between the SEA model and macroscopic quantities of the physical structure. The SEA model can be viewed as a set of non-negative numbers: the loss factors. They characterize the steady-state behaviour of the physical system over a certain frequency band. The macroscopic quantities are the average power injected into the subsystems, and the total energy stored in the subsystems. They correspond respectively to stimuli acting on the system and to the response of its various constituents. Finally, the link itself is linear.

Unfortunately, it is not yet known if the above expressions hold for groups of modes which differ substantially in terms of their internal damping, frequency distribution and coupling to other modes. Further progress in the analytical analysis of broad-band multimodal interactions is impeded by the unwieldiness of the expressions involved. Further experimental evidence is therefore highly desirable. In particular, a general experimental technique, which could determine the loss factors of specific resonant structures, would provide an objective test of SEA models. The development of such a technique has been the purpose of this project and its general principle is outlined in Section 2.3. The next section presents general comments about measuring the loss factors.

2.2 Measuring the Loss Factors

The loss factors cannot be measured directly. They are deduced from measurements of other quantities, such as reverberation time, total stored energy, power injected, power transmitted etc... It is therefore expected that experimental errors will combine in a cumulative fashion.

Given a single subsystem (i.e. a group of similar modes), the determination of the internal loss factor is, in principle, a simple matter. In steady-state, the measurement of the injected power P^{inj} and total stored energy E yields the internal loss factor η since

$$P^{inj} = \eta \ \omega_c \ E \qquad .$$

In a typical decay-rate situation,

$$\frac{dE}{dt} = - \eta \ \omega_c \ E \qquad .$$

A record of the decaying stored energy E provides η from the exponential rate of decay.

These apparently straight-forward procedures deserve further comments.

a) If the 'similar' modes of the subsystem have substantially different damping coefficients, the two approaches should in general yield different loss factors, unless the distribution of dissipated energy among the modes in the steady-state situation is identical to that in the 'average' decay-rate situation.

b) The measurement of injected power can prove quite a challenge, e.g. loudspeaker in a reverberant room.

c) It is not always easy to decipher a multimode decay-rate curve.

Consequently, is is not always quite clear which method should be used, and often the choice results from practical considerations.

Consider now several subsystems coupled together. This time, the energy balance equations contain several loss factors together. Decay-rate experiments lead to a linear system of first order differential

equations. Steady-state experiments lead to an algebraic system. A combination of both techniques has been suggested (Brooks and Maidanik, 1977) involving ratios of steady-state energies and ratios of decaying energies. A purely steady-state approach seems simpler to implement. Measurements of the steady-state injected powers and stored energies, for various power injection configurations, result in a linear algebraic system, which can theoretically be solved to find all the loss factors of the system under examination. Also, it seems more consistent to estimate steady-state quantities from steady-state situations, since it is not clear when the steady-state loss factors can be used in decay-rate situations and vice versa (Bies and Hamid, 1980). In some cases, one can isolate certain subsystems (e.g. by severing or blocking the other subsystems) in order to estimate the internal loss factors from measurements on a single system, but this is not always physically possible, nor justified.

In short, the so-called energy balance method, whereby all loss factors are determined from a steady-state energy balance system of equations, should provide an attractive and consistent approach to the determination of the steady-state SEA parameters.

Unfortunately, earlier attemps have lead to negative loss factors (a physical impossibility of course), probably because of experimental error accumulation (Lyon, 1975 p 218). In fact, to quote R.H. Lyon: "The procedure for parameter evaluation just described is not an established method... There is no reported analysis of the sensitivity of the derived parameter values to small errors in measured energy and input power values." The only successful evidence of this method was given by Hamid (Bies and Hamid, 1980 - Hamid, 1981). This evidence seemed sufficiently encouraging to justify a more systematic approach, involving in particular the design of a general experimental method and a sensitivity analysis. The next chapters are devoted to the presen-

tation of this work, while the basic principle is outlined in the next section.

2.3 Deduction of Loss Factors from Energy Balance Equations

The energy balance equations can be written in a general matrix form,

$$(E)\ (\eta) \ = \ (P/\omega_c)$$

For a system of order two, i.e. consisting of two subsystems:

$$\begin{bmatrix} E_1 & E_1 & -E_2 & 0 \\ 0 & -E_1 & E_2 & E_2 \end{bmatrix} \begin{bmatrix} \eta_{11} \\ \eta_{12} \\ \eta_{21} \\ \eta_{22} \end{bmatrix} = \begin{bmatrix} P_1/\omega_c \\ P_2/\omega_c \end{bmatrix} \qquad [1]$$

If one is to deduce the loss factors from measurements of E_1, E_2, P_1 and P_2, four linearly independent equations have to be constructed from the general case above. These four equations can result from two different power injection configurations. For a system of order N, N^2 linearly independent equations are required to determine the N^2 loss factors, thus N different power injection configurations must be analysed. The loss factors are the solutions of the linear algebraic system of N^2 equations. If the model has good physical significance, this system should never be ill-defined. However, the system results from experimental measurements of the injected powers P_i's and stored energies E_i's, and is therefore only an approximation to the actual system. Consequently, the solutions of that system are, in turn, approximations of the loss factors. The relative errors $\frac{\Delta\eta}{\eta}$ have the general form

$$\frac{\Delta\eta}{\eta} \ = \ a \ \frac{\Delta E}{E} \ + \ b \ \frac{\Delta P}{P}$$

where $\frac{\Delta E}{E}$ and $\frac{\Delta P}{P}$ are the relative errors on the average stored energies and the average injected powers respectively. The experimental

errors are amplified by the sensitivity coefficients a and b. These sensitivity coefficients are greater than unity and depend on the loss factors (they also depend on the experimental procedure, i.e. the power injection configuration.) This means that certain systems will be harder to analyse than others. In fact some systems might prove impossible to resolve, when the SEA model fails to represent the physical reality (Brooks and Maidanik, 1977). The sensitivity coefficients are derived in the next chapter for a system of order two.

Alternatively, system [1] can be solved for E_1 and E_2 and the relative errors on the average stored energies expressed thus

$$\frac{\Delta E}{E} = c \frac{\Delta \eta}{\eta} + d \frac{\Delta P}{P} \quad .$$

The new sensitivity coefficients c and d indicate how the response E of the system is affected by the characteristics of the system itself (i.e. the loss factors) and by the outside world (i.e. injected power). In other words, c and d determine whether or not the model is able to predict E accurately, given a knowledge $\frac{\Delta \eta}{\eta}$ and $\frac{\Delta P}{P}$ of the system. Note that here again, the sensitivity coefficients depend on the loss factors and the power injection configuration.

In summary, the loss factors can, theoretically, be obtained from the energy balance equations, provided that the injected power and stored energy can be measured for each subsystem. The limitation lies in the sensitivity coefficients which amplify the experimental errors.

...ooo000ooo...

EXPERIMENTAL PROCEDURE

3.1. The Basic Principle

Given a SEA system of order N (i.e. N subsystems), N^2 linearly independent energy balance equations are required to determine the N^2 loss factors from measurements of average broad-band injected powers and stored energies. Generally, one should measure N injected powers and N stored energies simultaneously, and this should be performed for N linearly independent situations. The latter condition is achieved by choosing N different power injection configurations.

A good choice for the N different power injection configurations is to inject power into only one subsystem at a time. Firstly, the N^2 energy balance equations obtained in this way are obviously linearly independent. Secondly, N - 1 input powers are known to be zero, and this leaves only one input power to be measured. Thirdly, if all input powers are equal to zero but one, only one stored energy and the non-zero injected power need be measured simultaneously. This is readily proved by noting that, although the values of the stored energies depend on the non-zero injected power, the distribution of these stored energies does not. Consequently, a power injection configuration, like the one just described, is fully investigated, simply by performing N dual measurements, each consisting of the non-zero input power together with a stored energy E_i, where i = 1, .. N.

For a system of order 2, the 4 linearly independent equations which result from the above method are:

$$\begin{bmatrix} E_{1\alpha}/P_{1\alpha} & E_{1\alpha}/P_{1\alpha} & -E_{2\beta}/P_{1\beta} & 0 \\ 0 & -E_{1\alpha}/P_{1\alpha} & E_{2\beta}/P_{1\beta} & E_{2\beta}/P_{1\beta} \\ E'_{1\gamma}/P'_{2\gamma} & E'_{1\gamma}/P'_{2\gamma} & -E'_{2\delta}/P'_{2\delta} & 0 \\ 0 & -E'_{1\gamma}/P'_{2\gamma} & E'_{2\delta}/P'_{2\delta} & E'_{2\delta}/P'_{2\delta} \end{bmatrix} \begin{bmatrix} \eta_{11} \\ \eta_{12} \\ \eta_{21} \\ \eta_{22} \end{bmatrix} = \begin{bmatrix} 1/\omega_c \\ 0 \\ 0 \\ 1/\omega_c \end{bmatrix} \qquad [2]$$

where the subscripts α,β,γ and δ refer to distinct experiments, the subscripts 1 and 2 refer to a subsystem, the non-primed quantities correspond to the power configuration $P_2 = 0$, and the primed quantities to the power configuration $P_1 = 0$.

It was the aim of this project to construct systems like system [2] for a given resonant structure. However, before dealing with the experimental aspects of this investigation, the next section is devoted to the sensitivity coefficients arising from system [2].

3.2. The Sensitivity Coefficients

For the purpose of this section, system [2] can be rewritten using a condensed notation:

$$\begin{bmatrix} E_1 & E_1 & -E_2 & 0 \\ 0 & -E_1 & E_2 & E_2 \\ E'_1 & E'_1 & -E'_2 & 0 \\ 0 & -E'_1 & E'_2 & E'_2 \end{bmatrix} \begin{bmatrix} \eta_{11} \\ \eta_{12} \\ \eta_{21} \\ \eta_{22} \end{bmatrix} = \begin{bmatrix} 1 \\ 0 \\ 0 \\ 1 \end{bmatrix} \qquad [3]$$

The solutions of system [3] are as follows:

$$\eta_{11} = \frac{E'_2 - E_2}{\Delta} \qquad \eta_{12} = \frac{E_2}{\Delta}$$

$$\eta_{21} = \frac{E'_1}{\Delta} \qquad \eta_{22} = \frac{E_1 - E'_1}{\Delta}$$

where $\Delta = E_1 E'_2 - E_2 E'_1$. The loss factors, η_{11}, η_{12}, η_{21} and η_{22} are greater than or equal to zero, and therefore

$$\Delta \geq 0 \; ; \qquad E'_2 \geq E_2 \; ; \qquad E_1 \geq E'_1 \; .$$

Consider a random variable x, a function of other random variables u,v,w etc....

$$x = f\,(u,v,w \ldots)$$

The variance of x, σ_x^2, can be approximated by (Bevington, 1969):

$$\sigma_x^2 \simeq \sigma_u^2 \left(\frac{\partial x}{\partial u}\right)^2 + \sigma_v^2 \left(\frac{\partial x}{\partial v}\right)^2 + \sigma_w^2 \left(\frac{\partial x}{\partial w}\right)^2 + \ldots.$$

$$+ 2\sigma_{uv}^2 \left(\frac{\partial x}{\partial u}\right)\left(\frac{\partial x}{\partial v}\right) + 2\sigma_{uw}^2 \left(\frac{\partial x}{\partial u}\right)\left(\frac{\partial x}{\partial w}\right) + 2\sigma_{vw}^2 \left(\frac{\partial x}{\partial v}\right)\left(\frac{\partial x}{\partial w}\right) + \ldots.$$

where σ_u^2, σ_v^2 and σ_w^2 are the variances of u, v and w, and σ_{uv}^2, σ_{uw}^2 and σ_{vw}^2 the covariances between u, v and w.

The 4 loss factors η_{11}, η_{12}, η_{21} and η_{22} are functions of 4 measured quantities: E_1, E_2, E'_1 and E'_2. These quantities are obtained by identical experimental procedures, and therefore present identical statistical characteristics:

$$\frac{\sigma_{E_1}^2}{E_1^2} = \frac{\sigma_{E_2}^2}{E_2^2} = \frac{\sigma_{E'_1}^2}{E'^2_1} = \frac{\sigma_{E'_2}^2}{E'^2_2} = \frac{\sigma_E^2}{E^2}$$

Moreover, these experiments are performed over different time intervals, and are therefore uncorrelated. Thus, the various covariances between the 4 random variables E_1, E_2, E'_1 and E'_2 are equal to zero. With these simplifications, the variances of the loss factors can be calculated, and their relative errors estimated as follows:

$$\sigma_{\eta_{ij}}^2 = \sigma_{E_1}^2\left[\frac{\partial \eta_{ij}}{\partial E_1}\right]^2 + \sigma_{E_2}^2\left[\frac{\partial \eta_{ij}}{\partial E_2}\right]^2 + \sigma_{E'_1}^2\left[\frac{\partial \eta_{ij}}{\partial E'_1}\right]^2 + \sigma_{E'_2}^2\left[\frac{\partial \eta_{ij}}{\partial E'_2}\right]^2$$

$$\sigma_{\eta_{ij}}^2 = \frac{\sigma_E^2}{E^2}\left[E_1^2\left[\frac{\partial \eta_{ij}}{\partial E_1}\right]^2 + E_2^2\left[\frac{\partial \eta_{ij}}{\partial E_2}\right]^2 + E'^2_1\left[\frac{\partial \eta_{ij}}{\partial E'_1}\right]^2 + E'^2_2\left[\frac{\partial \eta_{ij}}{\partial E'_2}\right]^2\right]$$

$$\frac{\sigma_{\eta_{ij}}^2}{\eta_{ij}^2} = \frac{\sigma_E^2}{E^2} \times \frac{1}{\eta_{ij}^2}\left[\ldots.\right]$$

$$\frac{\Delta\eta_{ij}}{\eta_{ij}} = \frac{\Delta E}{E} \times \frac{1}{\eta_{ij}}\left[\ldots.\right]^{1/2}$$

The sensitivity coefficients, S_{ij} are then given by

$$S_{ij} = \frac{1}{\eta_{ij}} \left[E_1^2 \left[\frac{\partial \eta_{ij}}{\partial E_1}\right]^2 + E_2^2 \left[\frac{\partial \eta_{ij}}{\partial E_2}\right]^2 + E_1'^2 \left[\frac{\partial \eta_{ij}}{\partial E_1'}\right]^2 + E_2'^2 \left[\frac{\partial \eta_{ij}}{\partial E_2'}\right]^2 \right]^{\frac{1}{2}}$$

Now define:

$$b_1 = \frac{\eta_{12}}{\eta_{11}} \qquad b_2 = \frac{\eta_{21}}{\eta_{22}}$$

These dimensionless parameters indicate the coupling strength (in the SEA sense) between one subsystem and the other. For each subsystem, they provide a measure of the relative importance between the average energy dissipated internally (as indicated by the internal loss factor η_{ii}), and the average energy transmitted to the other subsystem (as indicated by the coupling loss factor η_{ij}).

After some elementary (but tedious) algebra, the sensitivity coefficients are expressed thus:

$$S_{11} = \left\{ 1 + 2 \frac{b_1 (1 + b_1)\left[b_1 (1 + b_1) + b_2 (1 + b_2)\right]}{\left[(1 + b_1)(1 + b_2) - b_1 b_2\right]^2} \right\}^{\frac{1}{2}}$$

$$S_{22} = \left\{ 1 + 2 \frac{b_2 (1 + b_2)\left[b_1 (1 + b_1) + b_2 (1 + b_2)\right]}{\left[(1 + b_1)(1 + b_2) - b_1 b_2\right]^2} \right\}^{\frac{1}{2}}$$

$$S_{12} = S_{21} = \left\{ 1 + 2 \frac{(1 + b_1)(1 + b_2)\left[(1 + b_1)(1 + b_2) + b_1 b_2\right]}{\left[(1 + b_1)(1 + b_2) - b_1 b_2\right]^2} \right\}^{\frac{1}{2}}$$

S_{11}, S_{22} and $S_{12} = S_{21}$ are displayed in Figure 1 for a realistic range of values b_1 and b_2. Several interesting points arise from these results:

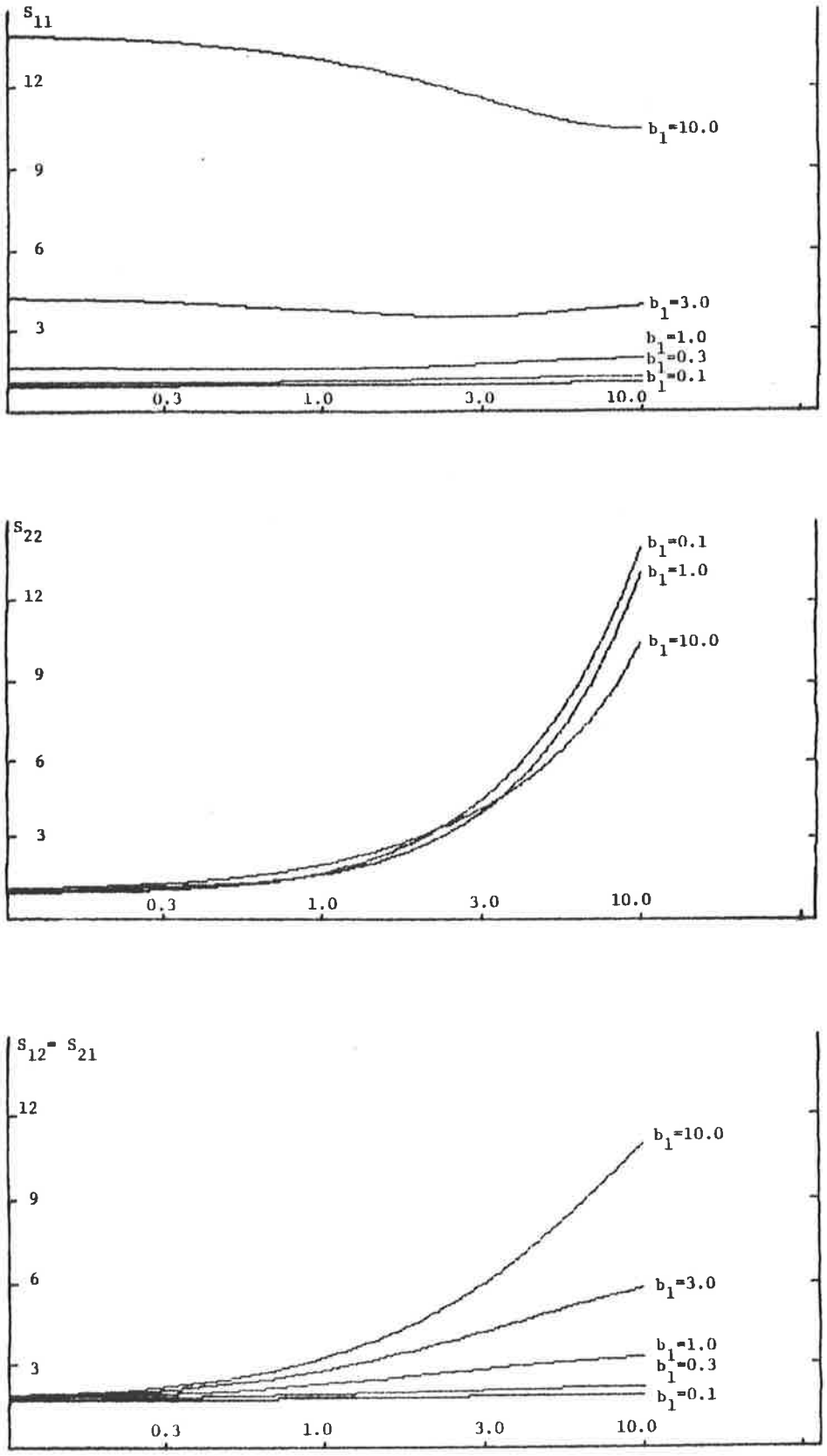

Fig. 1 Sensitivity Coefficients versus coupling strength b_2

$b_1 = \eta_{12} / \eta_{11}$ $b_2 = \eta_{21} / \eta_{22}$

a) S_{11} and S_{22} are always larger than 1.

b) $S_{12} = S_{21}$ is always larger than $\sqrt{3}$

c) The S_{ij}'s are small for b_1 and b_2 small. They are large for b_1 and b_2 large.

d) S_{11} is very sensitive to b_1 when b_1 is larger than 1. It is not sensitive to b_2, even for b_1 large. Similar results apply for S_{22}.

e) $S_{12} = S_{21}$ is sensitive to b_1 or b_2 only if b_1 and b_2 are larger than 1. Thus if b_1 or b_2 is small, $S_{12} = S_{21}$ remains small.

A general conclusion is that the loss factors of strongly coupled subsystems (i.e. b_1 and b_2 large) cannot be resolved. Also, if only one subsystem is strongly coupled, in the sense of having a large b, the corresponding internal loss factor has a much larger sensitivity coefficient than the other three loss factors.

Unfortunately, for systems with more than two subsystems, the analytical determination of the sensitivity coefficients becomes very cumbersome so that any generalization to N subsystems does not seem possible. A computer simulation might provide the answer, but this was beyond the scope of this project. However, the general trends, established for a system of order two, should prove useful when dealing with more complex systems.

3.3. A Description of the Experiments

3.3.1.

The experimental principle described in Section 3.1. was applied to a simple mechanical system under broad-band excitation. The system chosen consisted of two thin steel plates welded along two edges at right angles to each other (the system is described in Section 3.4). The two subsystems considered were the flexural modes of each plate,

taken from a frequency band $\Delta\omega$ centred at ω_c.

The stored energies were deduced from the mean transverse square acceleration, according to:

$$E = \frac{M \langle a^2(\omega) \rangle_{x,t}}{\omega^2}$$

where E is the average flexural energy stored in a thin homogeneous plate of mass M at a radian frequency ω, $\langle a^2(\omega) \rangle_{x,t}$ is the space and time average of the transverse square acceleration. $\langle a^2(\omega) \rangle_{x,t}$ was estimated from measurements of the transverse acceleration, using accelerometers, at m points spread randomly over the surface of the plates, according to:

$$\langle a^2(\omega) \rangle_{x,t} = \frac{1}{m} \sum_{i=1}^{m} \langle a_i^2(\omega) \rangle_t .$$

The injected powers P were deduced from the point-force f and point-acceleration a at the point of excitation, according to:

$$P = \langle f \, . \int a.dt \rangle_t \quad .$$

f and a were supplied by a force-acceleration transducer inserted between the electro-mechanical power source and the point of excitation on the plate. In order to obtain meaningful average quantities, power was successively injected at 5 different locations on each plate (Cremer and Heckl and Ungar, 1975 pp. 291-297).

3.3.2.

In a first attempt to measure the injected powers and stored energies, analog techniques were used. A substantial amount of time was devoted to this approach, but for reasons given below, it was eventually abandoned. It is therefore felt, that only a brief account of the techniques used, and the problems encountered, is justified.

The point-acceleration was integrated, then multiplied by the point-force to provide the instantaneous injected power. The square

transverse acceleration was simply obtained by squaring the transverse acceleration. Both operations (i.e. multiplying and squaring) were performed by AD 530 integrated circuits ('Analog Devices' series). The instantaneous injected power and square transverse acceleration were then time-averaged through long time-constant integrators. These slowly varying signals were then sampled and averaged by an Intel - 8080 microprocessor.

As one would expect, the main problem encountered was associated with the measurement of the injected power. The signal to noise ratio was rather poor after integration of the point-acceleration, even though the original, several milli-Volts strong, point-acceleration was first amplified, then integrated, and finally high-pass filtered. Also, the integrator introduced a small phase shift which could only be approximately compensated. In comparison, the point-force signal, typically one Volt strong, reached the multiplier in its original condition. There were other problems associated with this technique. From a practical viewpoint, the same experiment had to be repeated as many times as there were frequency bands of interest, since the frequency resolution was equal to the bandwidth of the injected power. Another repetition factor was imposed by the limited number of analog channels available. In short, the final result was a rather tedious and inaccurate procedure.

Nonetheless, this procedure was applied to the two-plate system described in Section 3.4. Eleven 1/3-Octave bands centred at 200 Hz, 250 Hz, 315 Hz, ... 1600 Hz and 2000 Hz were investigated. In these bands the mode count ranged from 20 modes in the 200 Hz band to 200 modes in the 2000 Hz band. On each plate, power was injected at 5 different locations and the transverse acceleration was measured at 16 different locations. The time averages were performed over 20 second intervals. Only 2 analog channels were available, one for the injected power and the other for a single transverse acceleration. Consequently,

19.6 hours of actual sampling were required. The energy balance equations obtained in this way are presented in Table 1, and the resulting loss factors in Table 2. Upon examination of Table 2, the 200 Hz and 250 Hz bands seem plausible. The 315 Hz, 400 Hz and 630 Hz bands appear rather doubtful in conjunction with the first two bands. The six remaining bands exhibit negative loss factors, without any distinct pattern, and were therefore definitely unsuccessful.

Clearly, there was room for improvement. The analog circuitry needed to be reviewed, with particular attention to low frequency noise and phase distortion. Also, more channels were required. However, the lack of flexibility in the frequency domain seemed unavoidable. These were serious obstacles to overcome, for possibly little benefit. It was therefore resolved to abandon the analog approach, and digital techniques were adopted.

3.3.3.

This new approach had many advantages over the previous one. The complex analog circuitry was replaced by a series of amplifiers, one for each channel. The amplified analog signals (the point-force, point-acceleration and transverse accelerations) were then digitized by a multi-channel data acquisition system. The spectra of the injected power and square transverse accelerations were obtained from these digitized signals by a series of computations. Since the spectral quantities were available, the frequency resolution could be made less than the bandwidth of the injected power, thus reducing considerably the required number of experiments.

The data acquisition and data processing system is described in Chapter 4, and its performance is analyzed in Chapter 5. It was applied to the test structure of Section 3.4, and loss factors were deduced successfully from the energy balance equations, over a frequency range of 5 Octave bands.

TABLE 1

ENERGY BALANCE EQUATIONS

1/3 - Octave Band [Hz]	E_1 [s] x 10	E_2 [s] x 10	E'_1 [s] x 10	E'_2 [s] x 10
200	3.07	1.92	1.79	3.89
250	2.45	1.43	1.55	3.20
315	3.47	2.66	3.34	3.44
400	3.10	1.94	2.90	3.06
500	2.86	1.58	3.30	2.58
630	2.43	1.36	1.49	4.11
800	1.81	2.82	0.79	2.24
1000	1.50	1.19	1.73	2.80
1250	1.38	1.22	10.37	5.52
1600	1.48	1.00	20.80	2.10
2000	1.45	1.28	6.85	2.78

N.B. Divide solutions by ω_c to find loss factors.

TABLE 2

LOSS FACTORS

1/3 - Octave Band [Hz]	η_{11} x 1000	η_{12} x 1000	η_{21} x 1000	η_{22} x 1000
200	1.9	1.8	1.7	1.2
250	2.0	1.6	1.7	1.0
315	1.3	4.4	5.6	0.21
400	1.1	2.0	3.0	0.22
500	1.4	2.3	4.8	X
630	0.87	0.43	0.47	0.30
800	X	3.1	0.87	1.1
1000	1.2	0.87	1.3	X
1250	X	X	X	2.3
1600	X	X	X	1.1
2000	X	X	X	0.94

N.B. a 'X' indicates a negative value.

3.4. A Description of the Test Structure

The test structure consisted of two rectangular thin steel plates welded along two edges, at right angles to each other. The plates are described in Table 3.

TABLE 3

Plate 1	Plate 2
Size : 1.2m x 1.2m	Size : 0.9m x 0.6m
Area : 1.44m^2	Area : 0.54m^2
Thickness : 1.00mm	Thickness : 0.40mm
Mass : 11.10 kg	Mass : 1.66 kg
Modal density : 0.49 mode/Hz	Modal density : 0.46 mode/Hz
Critical frequency : 12.7 kHz	Critical frequency : 31.8 kHz
Z_p : 89.80 kg/s *	Z_p : 14.37 kg/s *
Density : 7700 kg/m^3	Density : 7700 kg/m^3
c_L : 5050 m/s **	c_L : 5050 m/s **

* Z_p is the space and frequency-average point-input-impedance (Beranek, 1971). ** c_L is the speed of longitudinal waves.

The common join between both plates was 0.9m long and included one corner of plate 1 and one edge of plate 2. Two strings were attached to an edge of plate 1 in such a way as to have both plates hanging vertically. The plates were not constrained in any other way. The configuration is illustrated in Figure 2. Five holes were drilled at random in each plate to provide attachment points for the power injection device. Another 16 holes were drilled at random in each plate to provide attachment points for the accelerometers. By 'drilled at random' is meant that no specific location was chosen, although two criterions were used to determine the overall pattern. The first was that no two holes would be closer to each other than 10 cm. The second was that all holes

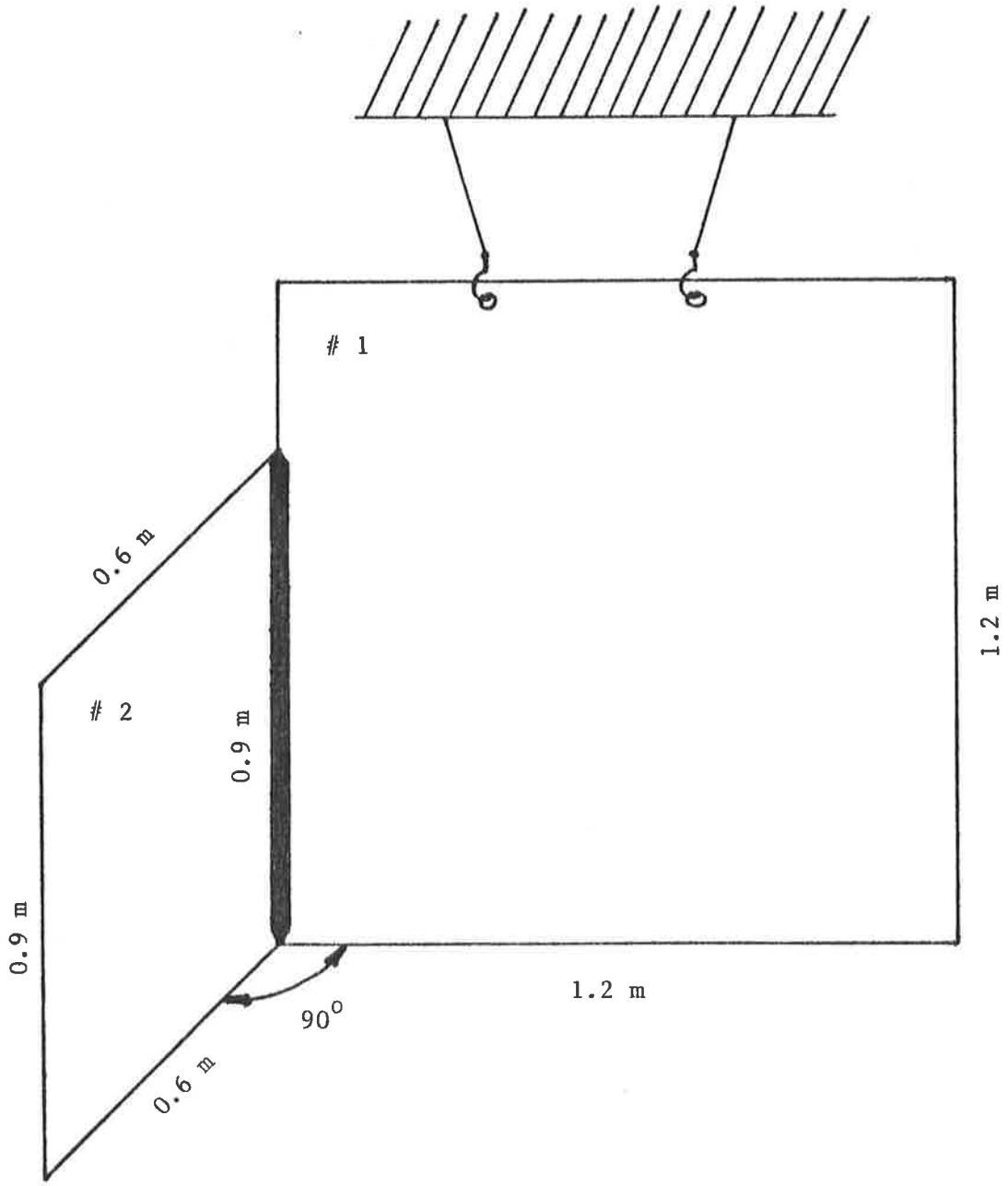

Fig. 2 Test-structure : two thin steel plates welded together
#1 is 1.0 mm thick
#2 is 0.4 mm thick

would be at least 10 cm away from the plate edges. All holes were 4 mm in diameter.

The accelerometers and the power injection device were bolted to the plates. Neither plate was artificially damped.

...ooo000ooo...

DATA ACQUISITION AND DATA PROCESSING

4.1. Analog Signals

Two physical quantities were to be measured simultaneously: the average broad-band point-injected power and the average broad-band stored energy. The injected power P was deduced from the point-force f_{tr} and point-acceleration a_{tr} sensed by the force-acceleration transducer. For a given radian frequency ω,

$$P(\omega) = < f_{tr}(\omega,t) \cdot \int a_{tr}(\omega,t) \cdot dt >_t$$

where $< >_t$ is a time-average quantity.

The stored energy E was estimated from the average of the transverse accelerations a_{pl-i} recorded on a plate as follows:

$$E(\omega) = \frac{M}{\omega^2} \frac{1}{m} \sum_{i=1}^{m} < a_{pl-i}^2(\omega,t) >_t .$$

M is the total mass of the corresponding plate. The plates were driven with white noise in octave bands centred at 125 Hz, 250 Hz, 500 Hz, 1 kHz and 2 kHz. It was considered that 8 transverse accelerations (i.e. m = 8) would provide an adequate average. Hence a total of 10 analog signals were considered with frequencies ranging from $\frac{125}{\sqrt{2}}$ = 88 Hz to 2000 x $\sqrt{2}$ = 2.8 kHz.

4.2. The Hardware

A 10-channel, 8-bit analog to digital (A/D) converter with a maximum sampling rate of 6250 Hz per channel was used to digitize the 10 analog signals. 8-bit accuracy was thought ample for the purpose, and 6250 Hz being greater than 2 times the highest frequency component (i.e. 2 x 2.8 kHz = 5.6 kHz), no aliasing resulted. The A/D converter was activated by a 16-bit word mini-computer: LSI - 11/02 with RT - 11 operating system. The total core memory available was 24 K words, (N.B. 1K = 1024 = 2^{10}) equivalent to 48 K samples by packing two 8-bit samples

in one word (i.e. one sample per byte). Mass storage was on single-sided double-density 8-inch floppy disks, each providing space for 10 times the core memory. For processing purposes, the data was copied from floppy disk to 9-track magnetic tape and transferred to the 60-bit word high-speed University computer: CYBER - 173 with a Network Operating System/Batch Environment (NOS/BE).

4.3. The Software †

4.3.1.

The spectra of the average injected power and the mean square acceleration were estimated from the time series, using a Fast Fourier Transform algorithm (FFT) in conjunction with a Kaiser-Bessel window. The Fast Fourier Transform is a well known approximation to the continuous Fourier Transform, and together with a Kaiser-Bessel window, 'leakage' is reduced to a minimum.

4.3.2.

The mean square acceleration spectrum is given by the power spectral density (PSD).

$$PSD(\omega) = \langle a_{pl}^{2}(\omega,t) \rangle_{t}$$

or

$$PSD(\omega) = \frac{1}{2} \; Re\{ A_{pl}(\omega) \cdot A_{pl}(\omega)^{*} \}$$

using the complex vector notation, and where '*' denotes the complex conjugate operator.

Consider X_p, p = 0,1... N-1 (N a power of 2), the FFT of x_m, m = 0,1... N-1, which is the time series obtained by sampling $a_{pl}(\omega,t)$. $A_{pl}(\omega)$ is approximated by X_p thus:

$$A_{pl}(o) = X_o \; ; \qquad A_{pl}(\Omega_p) = 2 X_p \qquad p = 1,2... N/2$$

$$\Omega_p = p \times \frac{f_s}{N} \qquad (f_s = \text{sampling rate})$$

It follows that:

† See Appendix for more details

$$PSD(o) = \frac{1}{2} \; Re \{A_{p1}(o) \; . \; A_{p1}(o)^*\} \; = \frac{1}{2} \; Re \{X_o \; . \; X_o^*\}$$

$$PSD(\Omega_p) = \frac{1}{2} \; Re \{ A_{p1}(\Omega_p) \; . \; A_{p1}(\Omega_p)^* \} \; = 2 \; Re \{X_p \; . \; X_p^*\}$$

X_p is computed using an N/2 - long FFT computation (Brigham, 1974 p. 169) at the expense of some rearranging of the results. Finally, $PSD(\Omega_p)$ is multiplied by a quantity called 'parseval', in order to satisfy Parseval's theorem which states that

$$\frac{1}{N} \sum_{m=0}^{N-1} | \; x_m \; |^2 \; = \; \frac{1}{N^2} \sum_{p=0}^{N-1} | \; X_p \; |^2 \quad ,$$

and to make up for the loss of energy imparted when windowing the signal. 'parseval' is then given by

$$\text{parseval} \; = \; \frac{1}{N^2} \; \frac{\sum_{m=0}^{N-1} | \; x_m |^2}{\sum_{m=0}^{N-1} | \; x_m \; . \; \text{window}(m) |^2}$$

where window(m) represents a value of the window function.

4.3.3.

The average injected power for a given radian frequency ω is

$$P(\omega) \; = \; < f_{tr}(\omega,t) \; . \; \int a_{tr}(\omega,t).dt >_t \quad .$$

This can be rewritten, using the complex vector notation and Fourier Transforms, with $j = \sqrt{-1}$

$$P(\omega) \; = \; \frac{1}{2} \; Re \{ F_{tr}(\omega) \; . \left[\frac{-j}{\omega} \; A_{tr}(\omega) \right]^* \}$$

Consider F_p and A_p, p = 0,1... N-1 (N a power of 2), the FFT's of f_m and a_m, m = 0,1... N-1 which are the time series obtained by sampling $f_{tr}(\omega,t)$ and $a_{tr}(\omega,t)$ respectively. $F_{tr}(\omega)$ and $A_{tr}(\omega)$ are approximated by F_p and A_p thus:

$$F_{tr}(o) = F_o \quad ; \qquad A_{tr}(o) = A_o$$

$$F_{tr}(\Omega_p) = 2F_p \quad ; \qquad A_{tr}(\Omega_p) = 2A_p \qquad p = 1,2\ldots N/2$$

$$\Omega_p = p \times \frac{f_s}{N}$$

It follows that,

$$P(\Omega_p) = \frac{1}{2} \text{ Re } \{2F_p \cdot (\frac{-j}{\Omega_p} \; 2 \; A_p)^* \} = 2 \text{ Re } \{F_p \cdot (\frac{-j}{\Omega_p} \; A_p)^* \}$$

$p = 1,2\ldots N/2$

F_p and A_p are computed from f_m and a_m, using <u>one</u> N-long FFT computation, at the cost of some sorting of the results (Brigham, 1974 p. 167). Finally $P(\Omega_p)$ is multiplied by (parseval 1 x parseval 2)$^{\frac{1}{2}}$ in order to satisfy Parseval's theorem, and to make good the loss of energy imparted when windowing the signals, where

$$\text{parseval 1} = \frac{1}{N^2} \frac{\sum_{m=o}^{N-1} | f_m |^2}{\sum_{m=0}^{N-1} | f_m \cdot \text{window}(m) |^2}$$

$$\text{parseval 2} = \frac{1}{N^2} \frac{\sum_{m=0}^{N-1} | a_m |^2}{\sum_{m=0}^{N-1} | a_m \cdot \text{window}(m) |^2}$$

4.3.4.

The choice of a particular window has a considerable influence on the final result of an FFT computation. Fundamental aspects were found in various texts on signal processing (Brigham, 1974 - Stanley, 1975 - Tretter, 1976). A very detailed review of data windows was given by Harris (Harris, 1978). Essentially, the best choice amounts to a reasonably narrow main-lobe and very small side-lobes. This is illustrated in Figure 3. One such window is the Kaiser-Bessel window,

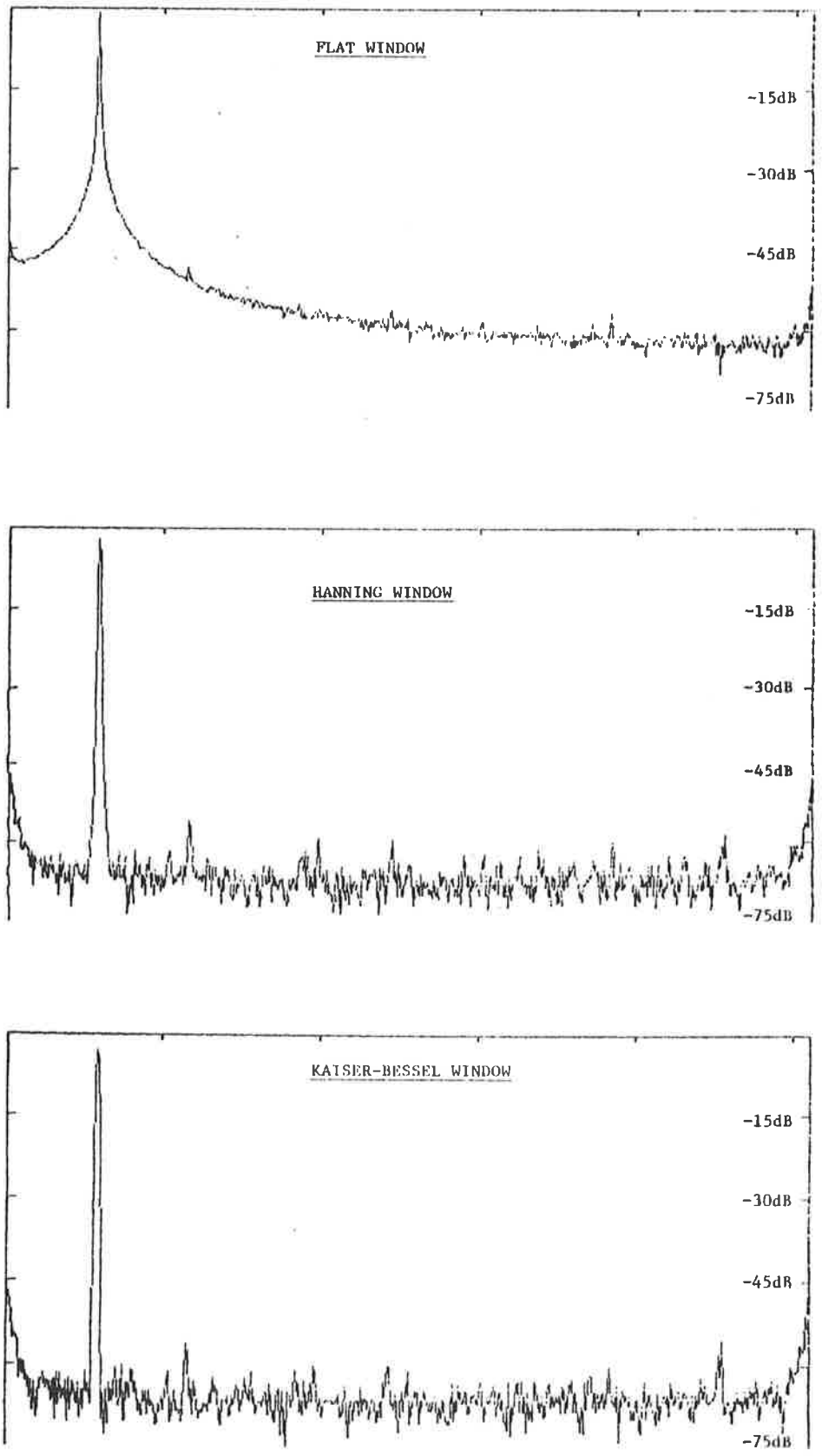

Fig. 3 FFT Power Spectrum for three different windows
5 × 1024 samples of 350 Hz sinewave at 6250 Hz

with a parameter of 3 (Harris, 1978 - Tretter, 1976). This window was used throughout this project.

4.3.5.

The modal density of a thin homogeneous plate does not depend on frequency. This motivated the choice of a constant frequency resolution. The width of one 'bin', or frequency point of an FFT spectrum, is given by $\frac{f_s}{N}$ where f_s is the sampling rate and N is the number of samples. Thus the highest constant frequency resolution was dictated by the largest number of samples, N_{max} (a power of two because of the FFT algorithm), compatible with the LSI -11/02 memory size. Bearing in mind that 48 K samples could be stored in the mini-computer, and that 10 channels were required, N_{max} was found equal to $2^{12} = 4096$. Consequently, time series as recorded in Table 4 were used. The width of one 'bin' was 1.5 Hz in all cases.

TABLE 4

Number of Samples N	Sampling Rate f_s [Hz]	Octave Band Centre Frequency [Hz]
4096	6250	2000
2048	3125	1000
1024	1560	500
512	780	250
256	390	125

Unfortunately, the width of one bin is far from being the frequency resolution of a spectrum derived from an FFT computation. Firstly, the window has a certain bandwidth, typically 3 bins (Harris, 1978). Secondly, owing to the random nature of the measured signals, and the poor variance of the FFT spectral estimator, many spectra computed from uncorrelated time series must be averaged in order to approach the mean with a reasonable degree of confidence. The number of such spectra can be reduced by grouping several bins together. Clearly a compromise must be sought, since a high frequency resolution and a small amount of data are mutually exclusive.

4.4. Computations†

Consider one time record as the sampling of the 10 channels: 1 time series for the transducer's point-force, 1 for the transducer's point-acceleration and 8 for the 8 transverse accelerations. The FFT's of the two time series from the transducer were combined in the frequency domain, as explained in section 4.3.3., to yield one FFT spectral estimate of the injected power. The PSD's of the 8 time series recorded on one plate, computed as outlined in section 4.3.2., were averaged to yield one FFT spectral estimate of the 8-point stored energy. Thus, one time record produced an estimate of both the injected power and the 8-point stored energy. A maximum resolution of 20 modes was thought appropriate, which meant that a minimum of 30 bins could be grouped together as each plate's modal density was about 0.5 mode/Hz. Even then, it was found that about 100 time records were required for the arithmetic averages of both spectral estimates to fall within 2.5% of their mean. Such a measurement of the injected power and 8-point stored energy (i.e. 100 time records) was referred to as one experimental point, when performed over the 5 Octave bands of interest. It was made up of 5 x 100 'time records', or 5 x 100 x 10 'time series'.

†See Appendix

The ratios of the stored energy spectrum over the corresponding injected power spectrum, were then averaged over the five driving points of each plate. This was done four times, as explained in the previous chapter (section 3.1), and the corresponding four spectra were used to generate one linear system of four equations for each frequency point. The solutions of one such system were the four loss factors which characterized the flow of energy over the corresponding frequency band (i.e. the band containing the bins which were grouped together).

The sequence of operations just described was implemented in six steps (some of the computer programs, written in PASCAL, are given in appendix):

1) Together with information relevant to the actual experiment (e.g. sampling rate, amplifier gains etc ...) 96 time records were collected on floppy disks for each Octave band in turn, using an LSI - 11/02 computer. This amounted to 7.6 Mbytes (one sample per byte) per experimental point, which fitted on 16 floppy disk sides. The computer time for one experimental point was about 55 mins, which included only 5 mins 16 secs of actual sampling, the difference being the time taken to write on disk. The 20 experimental points took a total of 18 hours 20 mins computer time and amounted to 152 Mbytes of data.

2) The raw data was copied from floppy disk to 9-track magnetic tape at a density of 800 BPI. One experimental point (7.6 Mbytes) fitted comfortably on a 2400-ft tape, using 512-byte blocks.

3) Each data tape was then copied (in duplicate) on the CYBER. Each copying operation used 18.5 secs CP (Central Processor) and about 27 mins 30 secs PP (Peripheral Processor). This step naturally required two tape units (this takes time on a multi-user system!).

4) Each experimental point was transferred from 9-track tape to the CYBER's mass storage, and the 16-bit 2's complement integers were converted to 60-bit integers in the process. Each transfer took 3 mins 51 secs CP and about 15 mins PP.

5) The time records were processed and averaged. Each experimental point took 1 hour 26 mins CP and about 18 mins 45 sec PP, giving a total of 28 hours 40 mins CP for the 20 points (this however, included the unpacking of the data).

6) The linear systems were constructed and solved.

The programs which performed these 6 steps were mainly written in PASCAL (cf. Appendix). Although the efficiency of the code generated by a present-day PASCAL compiler is not as good as, say, an optimised FORTRAN compiler, the computer times quoted above are representative of the amount of 'number crunching' required.

In spite of the many months spent to reach this particular hardware-software combination, it is believed that these computer times are only upper bounds of what can be done. Dedicated hardware, machine language, improved software techniques, faster processors etc .... offer attractive future improvements. Consequently, it seems appropriate to conclude this chapter by discussing some improvements which readily come to mind.

4.5. Discussion - Improvements

Step 1 - 2

Most of the time was spent outputting the sampled data to a storage medium. The total sampling time was less than 2 hours for the whole experiment (compare this with the $\frac{19.6}{2}$ hours of the 'analog method'). Thus a good 10-channel analog tape recorder could reduce the time spent 'in situ' to a few hours. The sampling device (i.e. the LSI - 11/02) could be fitted with a digital tape unit, thus avoiding the tedious replacement of floppy disks and suppressing step 2 entirely.

Step 3 - 4

512-byte blocks were used on all magnetic tapes. Longer blocks would improve the storage capacity of the tapes by reducing the number of IRG's (Inter Record Gaps). The unpacking and integer conversion could be written in machine language and performed together at this stage. This would probably reduce the processing times of step 5, which includes the unpacking, by as much as 25%.

Step 5

The essence of this step is to deduce spectral quantities accurately from the least amount of data in the shortest possible time. Using the FFT algorithm is a well-known, fast and efficient way of approximating the continuous Fourier Transform. A reputedly good window was used throughout the computations, namely a Kaiser-Bessel window. Unfortunately, when dealing with non-deterministic quantities, the number of uncorrelated time series required to reduce the variance of an FFT-based estimator is very large. The use of overlapping time series could reduce the amount of data significantly, provided that the overlapping records are almost uncorrelated. For instance, 50% overlap, and yet less than 10% correlation, can be achieved with a suitable window, e.g. Kaiser-Bessel 3 (Harris, 1978). In the case of the P.S.D., where the phase information is not needed in the frequency domain, the Maximum Entropy Method (MEM) could be used successfully. The Maximum Entropy Method provides a P.S.D. estimator of better variance and frequency resolution than its FFT counterpart (Haykin, 1978). However, the computation must be performed in real arithmetic, and this is a disadvantage if a high-speed computer is not available. The Maximum Entropy Method was never actually used when processing the data for this project, basically for two reasons. Firstly, the FFT algorithm is at present more familiar to the engineering community. Secondly, an FFT computation was required anyway to evaluate the injected power. However, the Maximum Entropy Method was considered at an earlier

stage, and deserves a brief mention here. A program† based on the comprehensive (and simple) flowchart by Andersen (Andersen, 1974), was developed to gain some understanding of this method. The power spectra obtained by MEM were smoother, with a better variance and accuracy than those obtained by FFT, especially when dealing with random signals. Figure 4 shows FFT and MEM at work on some simple signals.

Step 6

The ratios of the stored energy to the injected power, E/P, were averaged over the 5 driving locations of each plate in order to construct the energy balance equations. Instead, one could use the least squares principle to find the system which fits the set of data best (Bies and Hamid, 1980). This was tried on one of the five Octave bands, as explained in section 5.4. Differences of less than 10% in the loss factors resulted.

4.6. Summary

A digital method was developed to measure the spectra of the injected power and the 8-point stored energy. The method used the Fast Fourier Transform algorithm to compute the desired spectral quantities from sampled time series. It was applied to the two-plate structure of section 3.4. About 150 Mbytes of data were collected in 20 hours on a mini-computer, and processed in 30 hours on a high-speed computer. The data processing included 86,400 FFT computations. Consequently, large amounts of data and long computing times seem inevitable, and the practicability of the method clearly depends on the availability of fast data logging and data processing facilities. Hence it is hoped that the hardware and the software presented in this chapter, as an experimental tool, will provide an informative starting point for future investigations. Having now dealt with the implementation of this digital

†See Appendix

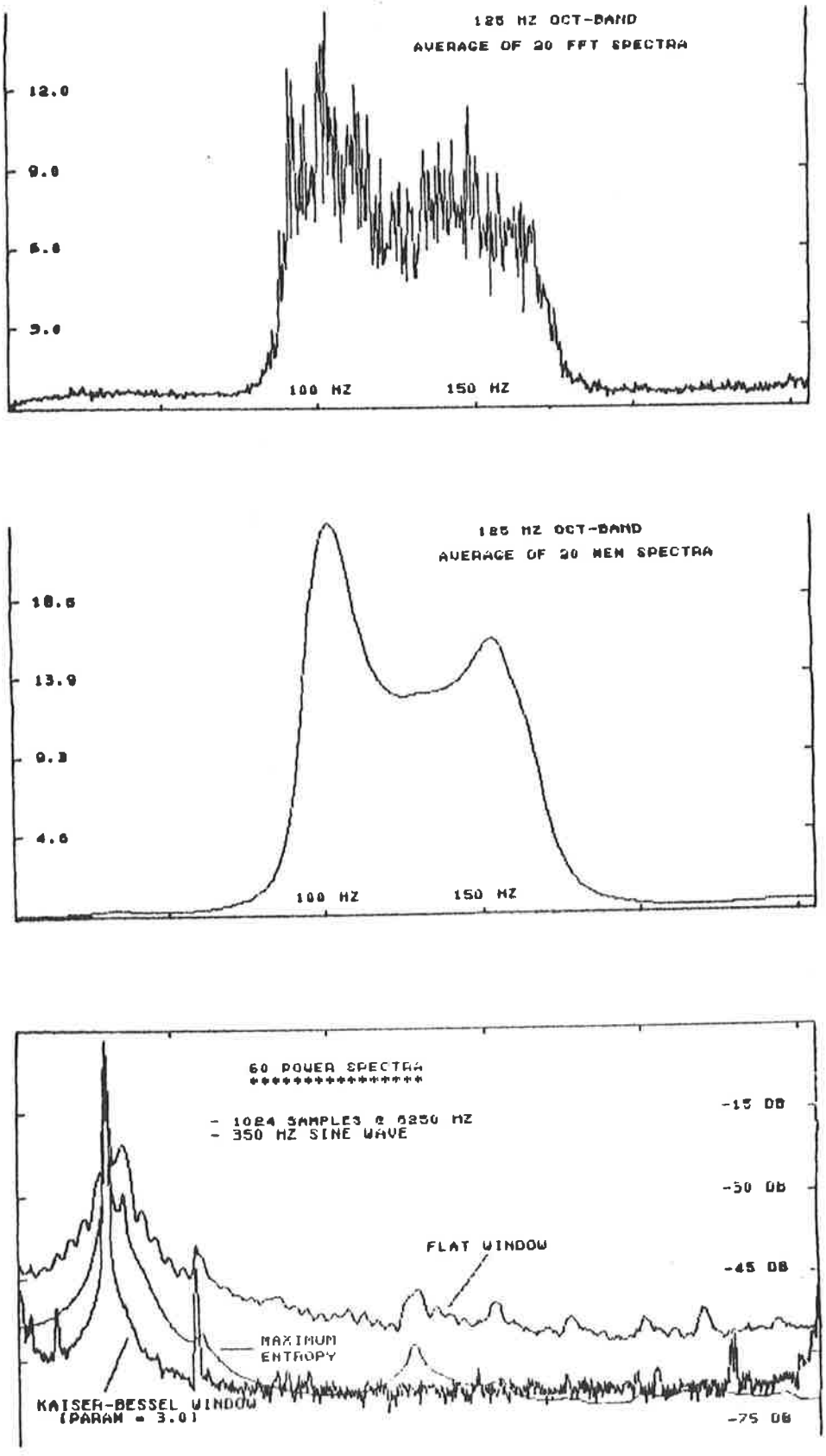

Fig. 4 Comparison of FFT and MEM Power Spectra

technique, the following chapter is dedicated to the examination of the quantitative results. In particular, the loss factors will be examined in detail.

...ooo000ooo...

EXPERIMENTAL RESULTS

5.1. Time Variance

As explained in the previous chapter (section 4.3.5.), given a frequency resolution, many uncorrelated spectral estimates must be averaged in order to achieve reasonable accuracy. The higher the desired frequency resolution, the larger the amount of data required.

The quantities measured on the test structure were of a random nature and their spectra exhibited resonant peaks. These two attributes were responsible for the large amount of data. A frequency resolution of 30 bins was chosen, which corresponded to 20 modes. This guaranteed a good statistical average of the modal quantities, without loosing much in terms of frequency resolution. The required amount of data was determined in the following manner. Power was injected into plate 1, and X time records were sampled on plate 1 for each of the five Octave bands, according to Table 4 of the previous chapter. After some computations (see section 4.4), X spectra of the power P injected into plate 1 and X spectra of the 8-point energy E stored in plate 1 were available, with about 25 - 30 bins grouped together. Consider A_m, the average of m uncorrelated spectra, then

$$\lim_{m \to \infty} \frac{| A_{m+1} - A_m |}{A_m} \times 100 = \lim_{m \to \infty} \delta_m = 0$$

or

$$\lim_{m \to \infty} A_m = A_{actual} \quad .$$

In other words, A_m is an asymptotically unbiased estimator. Table 5 presents the behaviour of δ_m corresponding to the averages of the X spectra of E and P for the five Octave bands. Taking a deviation of up to 5% as an acceptable error on the ratio E/P corresponds to the δ = 2.5% entry in Table 5. This determined the choice of about 100 time records.

TABLE 5

LAST RECORD m WITH DEVIATION δ

δ [%]	125 Hz Octave 26 bins together 190 time records		250 Hz Octave 26 bins together 141 time records		500 Hz Octave 27 bins together 184 time records		1000 Hz Octave 25 bins together 198 time records		2000 Hz Octave 25 bins together 190 time records	
	m(E)	m(P)	m(E)	m(P)	m(E)	m(P)	m(E)	m(P)	m(E)	m(P)
100	X	X	X	X	X	2	2	2	2	2
75	X	X	X	X	X	-	-	-	3	-
50	X	2	2	3	X	-	-	-	-	3
25	X	-	6	6	5	5	5	5	7	8
10	6	10	-	12	15	15	17	11	21	21
5.0	23	11	17	40	29	29	26	31	34	38
2.5	26	66	27	107	30	61	70	75	55	82
1.0	126	100	130	131	173	165	131	198	168	167

'X' : no record found for corresponding δ

'-' : no record found for corresponding δ, but a larger δ was recorded previously

5.2. Space Variance

Each plate of the test structure was driven at five different points. The energy balance equations were constructed from the four (2^2) average values of the corresponding five E/P ratios. As mentioned earlier, one might prefer to construct the linear system which fits the available data best, in the least squares sense. This approach will be examined briefly in a following section. Whichever way is chosen, five E/P ratios were determined experimentally, their only difference being the power injection location, and it is informative to examine the spread of these five ratios around their mean. Before however, it must be reminded that, given a frequency resolution of r bins the E/P ratios are given by

$$\frac{<E>_r}{<P>_r}$$

and not by

$$<\frac{E}{P}>_r$$

where $<>_r$ indicates that r bins are averaged together. The normalized standard deviations σ_o of the five E/P ratios are presented in Table 6, using the condensed notation of section 3.2. (see system [3], Chapter 3). $\sigma_o(x)$ being defined as follows:

$$\bar{x} = \frac{1}{m} \sum_{i=1}^{m} x_i$$

$$\sigma(x) = \left[\frac{1}{m} \sum_{i=1}^{m} (x_i - \bar{x})^2 \right]^{\frac{1}{2}}$$

$$\sigma_o(x) = \frac{\sigma(x)}{\bar{x}} \times 100 \quad .$$

5.3. The Loss Factors

5.3.1.

As a result of the experiments outlined in the previous chapters, the test structure's energy balance equations were determined over

TABLE 6.a.

20 modes (30 bins) together

Frequency [Hz]	$\sigma_o(E_1)$ [%]	$\sigma_o(E_2)$ [%]	$\sigma_o(E_1')$ [%]	$\sigma_o(E_2')$ [%]
110	8.1	6.3	14.1	12.2
155	3.8	12.2	8.8	17.1
199	9.7	28.3	14.6	14.2
243	14.3	10.6	19.9	11.9
287	5.1	9.4	22.6	15.9
331	9.6	12.5	16.5	18.4
376	19.7	23.2	11.4	9.6
420	6.1	18.3	9.7	16.8
464	18.3	18.1	10.8	18.4
508	7.5	11.4	18.3	16.7
552	15.0	7.7	18.9	17.7
597	15.9	9.5	28.5	16.0
641	21.6	13.0	26.3	14.7
685	10.3	* 32.4	* 30.1	** 42.9
731	17.8	16.4	28.4	18.2
778	17.3	* 36.0	* 37.4	25.5
825	20.7	17.8	27.2	** 51.3
872	26.5	20.8	** 43.2	* 39.4
919	* 39.1	24.3	* 33.5	* 32.9
966	22.5	21.4	21.7	* 32.8
1014	11.8	22.9	26.3	9.7
1061	13.5	21.0	13.3	12.7
1108	20.4	17.7	24.5	24.2
1155	15.7	11.7	4.0	11.3
1202	15.2	10.3	12.8	22.1
1249	14.8	4.8	22.4	14.3
1296	17.0	5.2	15.9	16.4
1344	17.8	13.7	14.0	26.1
1391	25.9	20.1	16.8	20.7
1436	13.0	13.9	7.1	* 30.0
1481	14.1	16.2	28.9	9.3
1525	6.0	17.8	* 30.0	7.9
1569	16.6	22.4	25.9	26.1
1613	15.5	5.8	15.6	17.1
1657	5.8	5.7	22.8	19.8
1701	27.6	4.3	8.6	27.3
1746	7.6	17.5	* 31.0	14.4
1790	21.5	9.5	19.4	21.2
1834	7.6	19.1	** 50.3	10.8
1878	18.0	17.6	21.9	17.3
1922	21.9	11.7	23.6	8.3
1967	16.1	17.0	11.2	25.7
2011	15.4	16.1	17.0	20.6
2055	13.6	21.5	19.0	16.1
2099	17.7	* 35.8	18.4	26.3
2143	* 36.2	19.7	8.7	26.6
2188	15.7	16.6	* 33.6	* 39.4
2232	12.6	7.1	20.6	6.0
2276	14.2	20.3	24.7	12.4
2320	* 34.1	7.5	20.4	26.5
2364	20.2	** 44.1	17.4	24.6
2409	14.4	13.0	** 40.3	22.5
2453	22.9	21.5	25.3	18.6
2497	10.7	26.0	8.9	22.2
2541	18.8	14.4	15.1	4.2
2585	28.7	20.4	22.4	19.5
2630	7.4	18.3	16.3	23.8
2674	24.7	20.2	21.1	21.2
2718	5.8	17.1	9.3	* 31.9
2762	14.6	20.7	26.2	26.6
2806	16.4	12.6	26.8	25.2

' * ' : between 30 and 40
'** ' : over 40

TABLE 6.b.

40 modes (60 bins) together

Frequency [Hz]	$\sigma_o(E_1)$ [%]	$\sigma_o(E_2)$ [%]	$\sigma_o(E'_1)$ [%]	$\sigma_o(E'_2)$ [%]
133	5.0	5.7	9.8	9.5
221	12.0	12.8	16.7	7.7
309	5.3	5.8	21.0	14.4
398	10.6	18.6	9.2	10.2
486	13.5	13.2	13.2	16.8
575	8.8	2.9	22.5	10.7
663	10.1	17.9	18.9	* 26.4
751	13.5	11.1	21.6	* 28.1
840	18.7	14.3	* 27.2	** 37.4
928	* 26.0	21.7	20.8	23.9
1016	13.9	15.7	13.8	13.7
1105	14.6	10.1	22.1	16.1
1193	10.4	9.0	11.1	11.0
1282	11.4	6.1	6.3	14.7
1370	15.0	12.8	5.7	15.6
1458	11.1	13.2	22.1	15.2
1547	10.0	16.6	16.9	18.7
1635	9.1	2.1	14.2	17.1
1724	17.7	12.2	14.1	15.7
1812	14.5	6.7	* 26.5	11.2
1900	19.0	8.0	18.8	9.7
1989	9.4	15.8	13.6	6.3
2077	14.3	* 26.2	11.3	14.8
2166	* 25.6	13.7	21.9	23.5
2254	9.7	9.5	20.7	7.5
2342	22.3	23.6	11.9	22.3
2431	18.6	16.7	** 30.0	14.7
2519	10.5	21.4	3.1	14.8
2607	16.2	6.9	11.4	19.2
2696	14.6	13.4	14.9	12.2
2784	11.5	14.5	18.6	16.9

' * ' : between 25 and 30

' ** ' : over 30

TABLE 6.c.

80 modes (120 bins) together

Frequency [Hz]	$\sigma_o(E_1)$ [%]	$\sigma_o(E_2)$ [%]	$\sigma_o(E'_1)$ [%]	$\sigma_o(E'_2)$ [%]
265	8.5	9.1	11.8	7.5
442	9.5	13.5	5.8	8.3
619	7.3	7.2	** 24.1	14.2
796	6.9	7.1	** 23.0	** 23.5
972	* 17.2	10.8	* 15.7	* 19.1
1149	10.4	7.9	12.8	7.9
1326	12.3	5.5	5.7	11.2
1503	9.7	9.1	13.5	* 15.6
1680	11.8	5.8	10.6	13.9
1856	10.3	5.4	** 23.3	8.4
2033	8.0	* 19.2	9.9	7.4
2210	14.8	9.7	* 18.4	14.3
2387	* 18.5	* 18.1	* 15.4	13.9
2563	4.0	12.9	5.6	4.6
2740	9.0	8.1	11.9	5.5

' * ' : between 15 and 20

' ** ' : over 20

the five Octave bands centred at 125 Hz, 250 Hz, 500 Hz, 1000 Hz and 2000 Hz. Groups of 20 modes were considered first (i.e. the maximum frequency resolution), then groups of 40 modes and 80 modes. The energy balance equations and the resulting loss factors are presented in Table 7 and 8 respectively. Note that the solutions of the energy balance equations (see system [3], Chapter 3) presented in Table 7 must be divided by ω_c, the centre radian frequency of the band, in order to obtain the loss factors of Table 8.

5.3.2.

The first point of interest was that the group size did not affect the loss factors substantially. The results obtained for 80 mode groups (Table 8.c) are approximately the arithmetic average of the results obtained for 40 mode groups (Table 8.b), and similarly, 40 mode groups correspond to the average of 20 mode groups (Table 8.a). The 80 mode group loss factors (Table 8.c) are presented graphically in Figure 5. Note the use of linear scales. A few remarkable points are apparent from Table 8 and Figure 5.

a) All loss factors have the same order of magnitude and do not exhibit a strong frequency dependence.

b) There are some negative results, but for η_{11} only (i.e. the internal loss factor of the large plate). Moreover, except for one isolated section, the negative values are concentrated in the 2000 Hz band.

c) The loss factors present a 'peak' in the 700 - 1000 Hz interval. η_{11} presents some negative values in this range.

d) η_{11} decreases steadily from 1.5×10^{-3} to 0.5×10^{-3} over the frequency range 125 - 1500 Hz, and is the smallest loss factor.

e) η_{22} does not diverge much from an average value of about 2.0×10^{-3} and is the largest loss factor.

TABLE 7.a.

ENERGY BALANCE EQUATIONS (20 modes together)

Frequency [Hz]	E_1[s]	E_2[s]	E'_1[s]	E'_2[s]
110	6.8	2.0	5.2	4.4
155	5.3	1.9	4.2	4.7
199	5.0	0.90	1.8	2.2
243	4.4	1.1	2.2	2.4
287	4.3	1.2	2.3	2.9
331	3.6	1.1	2.7	2.9
376	2.8	0.85	1.3	1.7
420	3.5	0.69	1.4	1.6
464	3.9	0.71	1.7	1.5
508	2.8	0.60	1.3	1.2
552	3.3	0.71	1.5	1.2
597	2.3	0.65	1.3	1.3
641	2.6	0.75	0.82	1.1
685	2.4	0.67	0.43	0.85
731	2.4	0.64	0.24	0.31
778	2.6	0.91	0.44	0.37
825	2.8	0.74	0.34	0.74
872	1.9	0.59	0.80	0.89
919	1.7	0.40	0.60	0.39
966	1.4	0.46	0.86	0.58
1014	1.5	0.54	0.66	0.69
1061	1.8	0.48	0.76	0.71
1108	2.1	0.56	0.83	0.94
1155	1.6	0.62	0.65	0.75
1202	1.8	0.58	0.68	0.79
1249	1.6	0.55	0.61	0.67
1296	2.1	0.67	0.52	0.79
1344	1.9	0.45	0.47	0.55
1391	2.0	0.59	0.62	0.58
1436	1.7	0.39	0.45	0.65
1481	1.7	0.43	0.62	0.50
1525	1.6	0.48	0.52	0.42
1569	1.8	0.56	0.40	0.66
1613	1.5	0.57	0.55	0.55
1657	1.5	0.46	0.38	0.43
1701	2.0	0.50	0.45	0.45
1746	1.8	0.62	0.32	0.51
1790	1.8	0.57	0.30	0.47
1834	1.7	0.44	0.31	0.46
1878	1.3	0.47	0.27	0.41
1922	1.7	0.48	0.29	0.36
1967	1.5	0.53	0.40	0.43
2011	1.5	0.52	0.39	0.50
2055	1.1	0.65	0.31	0.39
2099	1.2	0.55	0.28	0.41
2143	1.2	0.44	0.33	0.46
2188	0.90	0.50	0.38	0.53
2232	0.97	0.68	0.30	0.59
2276	0.82	0.50	0.26	0.48
2320	0.99	0.61	0.33	0.50
2364	1.2	0.63	0.29	0.54
2409	1.1	0.53	0.30	0.41
2453	1.0	0.78	0.20	0.52
2497	1.1	0.70	0.32	0.50
2541	1.0	0.49	0.23	0.40
2585	0.91	0.63	0.26	0.40
2630	1.0	0.57	0.23	0.45
2674	0.92	0.66	0.21	0.60
2718	1.1	0.55	0.18	0.46
2762	0.91	0.79	0.16	0.43
2806	1.1	0.60	0.25	0.39

TABLE 7.b.

ENERGY BALANCE EQUATIONS (40 modes together)

Frequency [Hz]	E_1 [s]	E_2 [s]	E'_1 [s]	E'_2 [s]
133	6.3	1.9	4.8	4.4
221	4.8	0.95	2.0	2.3
309	4.1	1.2	2.5	2.9
398	3.2	0.78	1.4	1.6
486	3.5	0.68	1.5	1.4
575	2.8	0.67	1.4	1.2
663	2.5	0.72	0.58	0.98
751	2.5	0.73	0.34	0.36
840	2.4	0.67	0.44	0.68
928	1.5	0.43	0.64	0.45
1016	1.6	0.50	0.78	0.67
1105	2.0	0.58	0.77	0.90
1193	1.6	0.57	0.68	0.74
1282	2.0	0.61	0.55	0.70
1370	1.9	0.50	0.52	0.56
1458	1.7	0.41	0.57	0.56
1547	1.7	0.52	0.47	0.54
1635	1.6	0.53	0.47	0.50
1724	1.9	0.56	0.37	0.48
1812	1.8	0.50	0.30	0.47
1900	1.5	0.57	0.28	0.39
1989	1.5	0.53	0.39	0.46
2077	1.2	0.60	0.30	0.40
2166	1.1	0.47	0.36	0.51
2254	0.90	0.60	0.28	0.54
2342	1.1	0.62	0.31	0.52
2431	1.0	0.67	0.26	0.47
2519	1.1	0.61	0.28	0.45
2607	0.98	0.60	0.25	0.42
2696	0.99	0.61	0.20	0.54
2784	1.0	0.72	0.20	0.42

TABLE 7.c.

ENERGY BALANCE EQUATIONS (80 modes together)

Frequency [Hz]	E_1 [s]	E_2 [s]	E'_1 [s]	E'_2 [s]
265	4.6	1.0	2.0	2.4
442	3.3	0.74	1.4	1.5
619	2.7	0.69	1.0	1.1
796	2.4	0.69	0.37	0.45
972	1.6	0.45	0.68	0.51
1149	1.8	0.57	0.72	0.82
1326	2.0	0.57	0.54	0.64
1503	1.7	0.48	0.51	0.55
1680	1.7	0.54	0.42	0.49
1856	1.7	0.49	0.29	0.43
2033	1.4	0.58	0.35	0.43
2210	0.99	0.53	0.32	0.52
2387	1.1	0.64	0.29	0.50
2563	1.0	0.61	0.26	0.44
2740	1.0	0.65	0.20	0.49

TABLE 8.a.

LOSS FACTORS (20 modes together)

Frequency [Hz]	η_{11} x 1000	η_{12} x 1000	η_{21} x 1000	η_{22} x 1000
110	1.8	1.5	3.8	1.2
155	1.7	1.1	2.6	0.65
199	1.1	0.78	1.6	2.7
243	1.1	0.85	1.7	1.7
287	0.97	0.67	1.3	1.1
331	1.2	0.73	1.7	0.58
376	0.96	1.0	1.6	1.8
420	0.73	0.56	1.2	1.7
464	0.58	0.55	1.3	1.7
508	0.69	0.75	1.6	1.9
552	0.46	0.72	1.4	1.9
597	0.85	0.80	1.7	1.1
641	0.40	0.84	0.92	1.9
685	0.24	0.90	0.57	0.26
731	-1.2	2.4	0.91	7.9
778	-1.9	3.3	1.6	7.9
825	*	0.78	0.37	2.6
872	0.43	0.87	1.2	1.7
919	**	1.7	2.5	4.5
966	0.45	1.7	3.2	2.2
1014	0.35	1.2	1.5	1.9
1061	0.37	0.77	1.2	1.7
1108	0.35	0.52	0.78	1.2
1155	0.22	1.0	1.1	1.7
1202	0.26	0.73	0.86	1.5
1249	0.20	0.97	1.1	1.7
1296	0.11	0.61	0.48	1.5
1344	0.14	0.65	0.68	2.1
1391	***	0.84	0.89	2.0
1436	0.30	0.46	0.52	1.5
1481	0.12	0.83	1.2	2.0
1525	-0.17	1.3	1.4	2.7
1569	0.11	0.58	0.42	1.5
1613	-0.04	1.0	0.99	1.8
1657	-0.05	0.90	0.74	2.3
1701	-0.08	0.72	0.65	2.2
1746	-0.14	0.78	0.40	1.9
1790	-0.13	0.75	0.40	2.0
1834	0.02	0.60	0.41	1.9
1878	-0.12	0.97	0.56	2.1
1922	-0.21	0.83	0.51	2.5
1967	-0.18	0.98	0.75	2.0
2011	-0.03	0.74	0.54	1.6
2055	-0.94	2.3	1.1	2.7
2099	-0.31	1.2	0.61	2.1
2143	0.03	0.77	0.57	1.6
2188	0.09	1.2	0.96	1.3
2232	-0.15	1.3	0.56	1.3
2276	-0.05	1.3	0.69	1.5
2320	-0.26	1.4	0.76	1.5
2364	-0.14	0.97	0.45	1.3
2409	-0.26	1.2	0.67	1.8
2453	-0.47	1.4	0.36	1.4
2497	-0.40	1.4	0.64	1.5
2541	-0.19	1.0	0.47	1.7
2585	-0.70	2.0	0.82	2.0
2630	-0.22	1.0	0.41	1.5
2674	-0.09	0.97	0.31	1.0
2718	-0.14	0.84	0.27	1.3
2762	-0.77	1.7	0.35	1.6
2806	-0.41	1.2	0.49	1.7

* $\eta_{11} = 2.0 \times 10^{-6}$

** $\eta_{11} = -3.6 \times 10^{-5}$

*** $\eta_{11} = -1.2 \times 10^{-5}$

TABLE 8.b.

LOSS FACTORS (40 modes together)

Frequency [Hz]	η_{11} x 1000	η_{12} x 1000	η_{21} x 1000	η_{22} x 1000
133	1.6	1.3	3.1	0.98
221	1.1	0.76	1.6	2.3
309	1.0	0.67	1.4	0.92
398	0.83	0.76	1.3	1.8
486	0.60	0.59	1.3	1.7
575	0.62	0.73	1.5	1.5
663	0.31	0.85	0.69	2.3
751	-1.2	2.4	1.1	7.1
840	0.02	0.94	0.62	2.8
928	0.10	1.7	2.6	3.7
1016	0.39	1.1	1.8	1.9
1105	0.35	0.64	0.85	1.3
1193	0.27	0.91	1.1	1.6
1282	0.10	0.69	0.63	1.7
1370	0.08	0.72	0.74	2.0
1458	0.22	0.64	0.88	1.7
1547	0.03	0.81	0.73	1.9
1635	-0.06	0.98	0.87	2.0
1724	-0.11	0.74	0.49	2.0
1812	-0.04	0.65	0.39	1.9
1900	-0.16	0.87	0.52	2.3
1989	-0.10	0.83	0.62	1.8
2077	-0.54	1.6	0.79	2.3
2166	0.07	0.93	0.71	1.4
2254	-0.13	1.3	0.61	1.4
2342	-0.20	1.2	0.57	1.4
2431	-0.42	1.4	0.53	1.6
2519	-0.31	1.2	0.55	1.6
2607	-0.41	1.4	0.56	1.7
2696	-0.10	0.87	0.28	1.1
2784	-0.64	1.5	0.42	1.7

TABLE 8.c.

LOSS FACTORS (80 modes together)

Frequency [Hz]	η_{11} x 1000	η_{12} x 1000	η_{21} x 1000	η_{22} x 1000
265	0.93	0.69	1.4	1.7
442	0.71	0.65	1.2	1.7
619	0.48	0.76	1.1	1.9
796	-0.58	1.7	0.89	4.9
972	0.19	1.5	2.3	3.0
1149	0.32	0.75	0.93	1.4
1326	0.09	0.70	0.66	1.8
1503	0.11	0.75	0.80	1.8
1680	-0.08	0.85	0.65	2.0
1856	-0.08	0.73	0.44	2.0
2033	-0.25	1.1	0.69	2.0
2210	-0.01	1.1	0.66	1.4
2387	-0.28	1.3	0.56	1.5
2563	-0.34	1.3	0.54	1.6
2740	-0.26	1.1	0.32	1.3

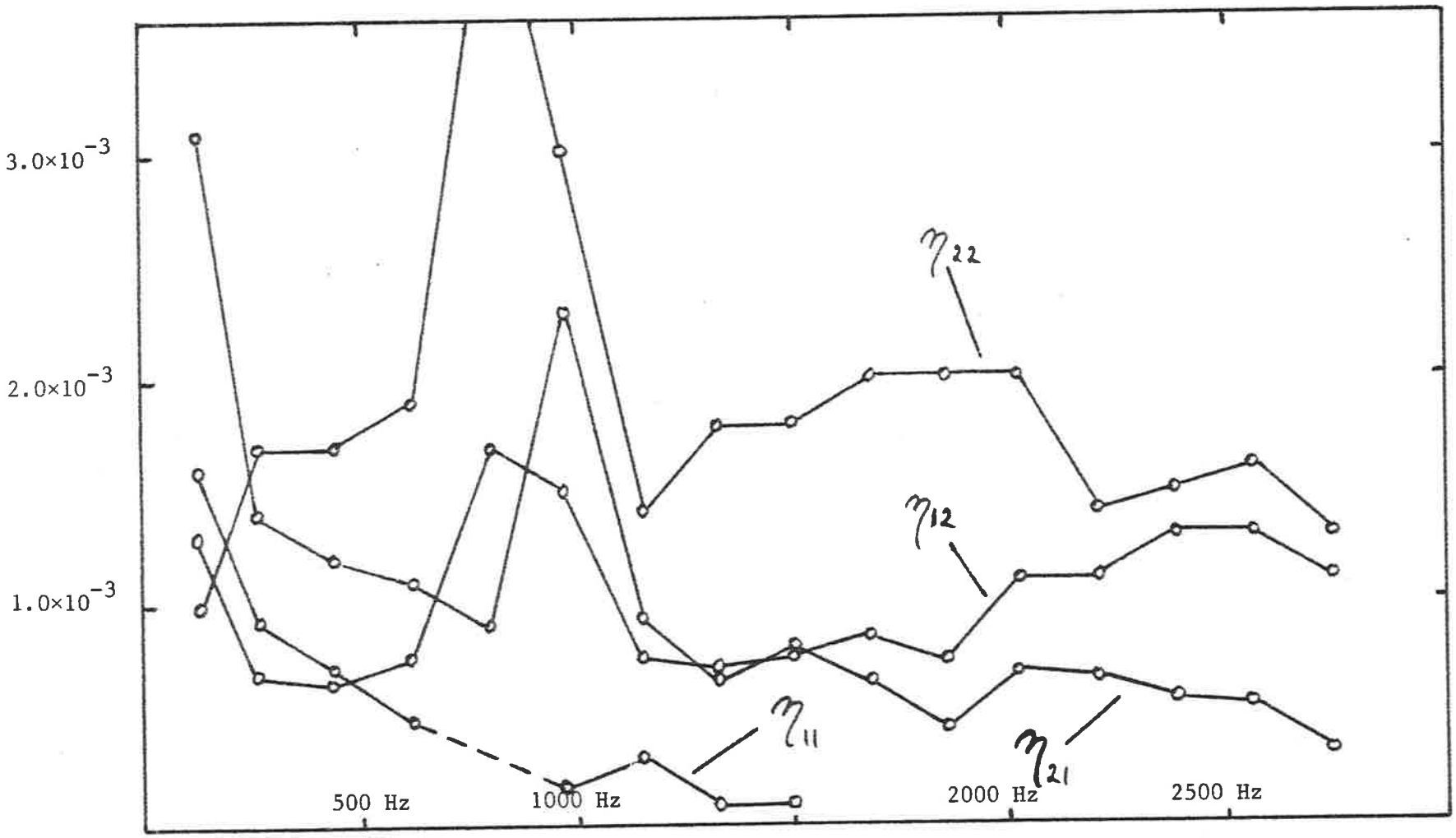

Fig. 5 Loss factors measured 'in situ' on test-structure

f) η_{12} has a small upward trend with frequency, and η_{21} a small downward trend. They 'meet' between 1200 Hz and 1700 Hz.

5.3.3.

It was shown in Chapter 3 how sensitivity coefficients of the various loss factors depended on the following two parameters (see Figure 1, Chapter 3):

$$b_1 = \frac{\eta_{12}}{\eta_{11}} \qquad b_2 = \frac{\eta_{21}}{\eta_{22}} \quad .$$

Examination of Figure 5 shows that b_2 is approximately equal to 0.5. b_1 is approximately equal to 1.0 for frequencies lower than 700 Hz, and approximately equal to 5.0 for higher frequencies. At frequencies where spurious results were obtained for η_{11}, it is highly probable that b_1 is also larger than unity. Of course, the loss factors of Figure 5 are estimates of the actual loss factors, distorted by experimental errors, and amplified by the actual sensitivity coefficients. Using these estimates to deduce sensitivity coefficients will naturally yield only approximate values. However, these approximate values lead to the interesting conclusion that η_{11} has a much larger sensitivity coefficient than the other three loss factors (see Figure 1, Chapter 3). This large sensitivity coefficient and the fact that a significant systematic error was introduced in the 2000 Hz band (see A/D converter in Appendix), explain why spurious results were obtained for η_{11} only, and why they were concentrated in the 2000 Hz band.†

5.4. The Radiation Loss Factor

The radiation loss did not contribute significantly to the total internal loss. This is readily verified by computing the radiation loss η_{rad} for each plate and comparing it with the internal loss factors deduced from the energy balance equations. η_{rad} is obtained from the coupling loss factor between a panel and an infinite

† See also section 5.6

acoustic space as follows (Lyon, 1975 p. 300):

$$\eta_{rad}(\omega) = \frac{R_{rad}(f)}{\omega M}$$

where ω is the radian frequency, f is the frequency, R_{rad} is the radiation resistance, M is the total mass of the panel. For $f < f_c$ (the critical frequency), R_{rad} is given by

$$R_{rad}(f) = \frac{4 \rho c \lambda_c P}{\pi^2} \beta \sin^{-1}(f/f_c)^{\frac{1}{2}}$$

where ρ is the density of air, c is the speed of sound in air, λ_c is the wavelength at the critical frequency f_c, P is the perimeter of the panel, β is a coefficient taken equal to 1 for a free panel. The critical frequency f_c is approximated by

$$f_c \simeq \frac{12500}{\text{thickness[mm]}} \quad [\text{Hz}] \ .$$

The radiation losses obtained from these expressions are shown in Table 9. They are smaller than the total internal loss factors by one order of magnitude.

TABLE 9

Radiation Loss Factors

Frequency [Hz]	$\eta_{11\text{-rad}}$	$\eta_{22\text{-rad}}$
125	2.7×10^{-4}	2.8×10^{-4}
250	1.9×10^{-4}	2.0×10^{-4}
500	1.3×10^{-4}	1.4×10^{-4}
1000	9.5×10^{-5}	1.0×10^{-4}
2000	6.9×10^{-5}	7.1×10^{-5}

5.5. The Theoretical Coupling Loss Factors

Wave-transmission calculations provide theoretical estimates of the coupling loss factors. The coupling loss factor between two joined plates is given by (Ødegaard Jensen, 1976):

$$\eta_{ij} = \frac{c_{gi} \; L_{ij}}{\omega \; \pi \; S_i} \; x \; \tau_{ij}$$

where c_{gi} is the group velocity in plate i, L_{ij} is the length of the junction between plates i and j, S_i is the area of plate i, and τ_{ij} is the transmission efficiency between plates i and j across the junction. For a homogeneous plate of rectangular cross-section, c_{gi} is approximately given by (Cremer and Heckl and Ungar, 1973):

$$c_{gi} \simeq 2 \; (1.8 \; c_L \; t_i \; f)^{\frac{1}{2}}$$

where c_L is the speed of longitudinal waves, t_i is the thickness of the plate and f the frequency.

Clearly, such calculation of the coupling loss factor depends on how τ_{ij} is estimated. The test-structure had a right-angle corner junction (see section 3.4). In first approximation, a wave normally incident to the junction was considered. However, this normal incidence transmission efficiency $\tau_{ij}(o)$ can be a rather primitive estimate (Plunt, 1980). A better estimate (or at least more sophisticated) is the average transmission efficiency across the junction $\overline{\tau_{ij}}$, where the average is taken over all possible angles of incidence. $\overline{\tau_{ij}}$ is computed thus:

$$\overline{\tau_{ij}} = \int_0^1 \tau_{ij}(\theta) \; . \; d(\sin\theta) \qquad [4]$$

where $\tau_{ij}(\theta)$ is the oblique incidence transmission efficiency for an angle of incidence θ. After some lengthy computations, Cremer and Heckl arrived at the following expression (Cremer and Heckl and Ungar,

1973, p. 401):

$$\tau_{ij}(\theta) = \frac{2\Psi_{ij}\left[(\kappa_{ij}^2 - s^2)(1 - s^2)\right]^{\frac{1}{2}}}{\Psi_{ij}^2 + \Psi_{ij}\{\left[(\kappa_{ij}^2 + s^2)(1 + s^2)\right]^{\frac{1}{2}} + \left[(\kappa_{ij}^2 - s^2)(1 - s^2)\right]^{\frac{1}{2}}\} + \kappa_{ij}^2}$$

where $s = \sin\theta$. If the panels i and j are made of the same homogeneous substance,

$$\kappa_{ij}^2 = \frac{t_i}{t_j} \qquad \text{and} \qquad \Psi_{ij} = \left[\frac{t_j}{t_i}\right]^2$$

where t_i and t_j are the thicknesses of panels i and j respectively.

$\overline{\tau_{ij}}$ was evaluated from equation [4] on a pocket calculator, using Simpson's rule. Note that the integrand is zero for angles larger than the total reflection angle. The results are presented in Table 10.

TABLE 10

Transmission Efficiency

$t_1 = 1.0 \times 10^{-3}$m ; $t_2 = 0.4 \times 10^{-3}$ m

$\kappa_{12}^2 = 2.5$; $\Psi_{12} = 0.16$; $\tau_{12}(o) = 0.167$; $\overline{\tau_{12}} = 0.124$

$\kappa_{21}^2 = 0.4$; $\Psi_{21} = 6.25$; $\tau_{21}(o) = 0.167$; $\overline{\tau_{21}} = 0.0785$

The theoretical coupling loss factors were given by:

$$\eta_{12} = 1.92 \times 10^{-1} \times \tau_{12} \times \frac{1}{\sqrt{f}}$$

$$\eta_{21} = 3.23 \times 10^{-1} \times \tau_{21} \times \frac{1}{\sqrt{f}} \quad .$$

These are tabulated in Table 11 for both normal ($\eta_{12}^{\perp}$ and $\eta_{21}^{\perp}$) and average oblique incidence ($\eta_{12}^{\not}$ and $\eta_{21}^{\not}$). The theoretical coupling loss factors are compared with those deduced from the energy balance equations in Figure 6. The agreement is striking between η_{21} measured in situ and η_{21} calculated for an average oblique incidence (except for the

TABLE 11

THEORETICAL COUPLING LOSS FACTORS

Frequency [Hz]	$\eta_{12}^{\perp}$ x 1000	$\eta_{21}^{\perp}$ x 1000	$\eta_{12}^{/}$ x 1000	$\eta_{21}^{/}$ x 1000
133	2.8	4.7	2.1	2.2
265	2.0	3.3	1.5	1.6
442	1.5	2.6	1.1	1.2
619	1.3	2.2	0.96	1.0
796	1.1	1.9	0.84	0.90
972	1.0	1.7	0.76	0.81
1149	0.94	1.6	0.70	0.75
1326	0.88	1.5	0.65	0.70
1503	0.83	1.4	0.61	0.65
1680	0.78	1.3	0.58	0.62
1856	0.74	1.3	0.55	0.59
2033	0.71	1.2	0.53	0.56
2210	0.68	1.1	0.51	0.54
2387	0.66	1.1	0.49	0.52
2563	0.63	1.1	0.47	0.50
2740	0.61	1.0	0.45	0.48

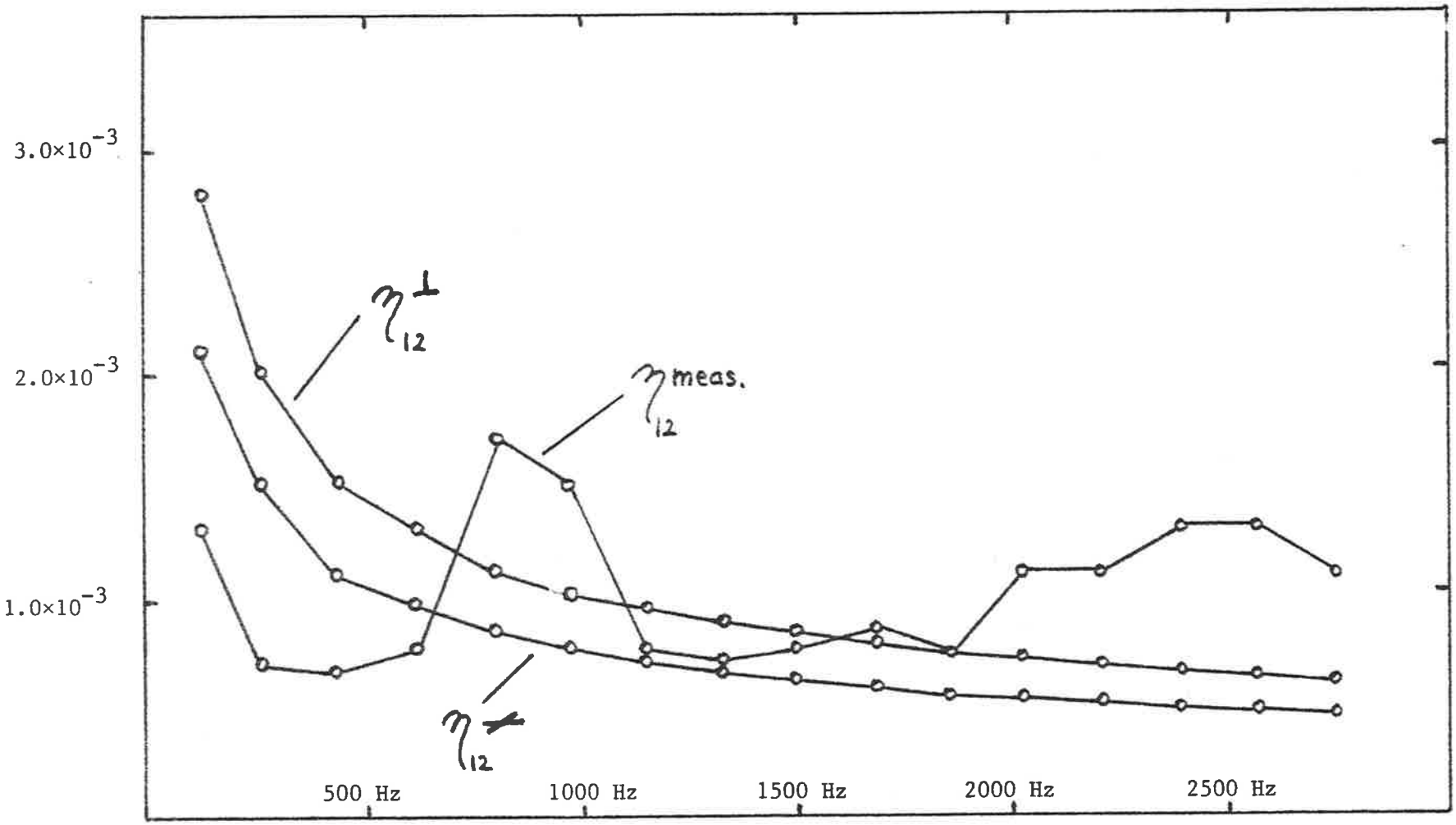

Fig. 6a Coupling loss factor measured 'in situ' and theoretical prediction for normal incidence and average oblique incidence

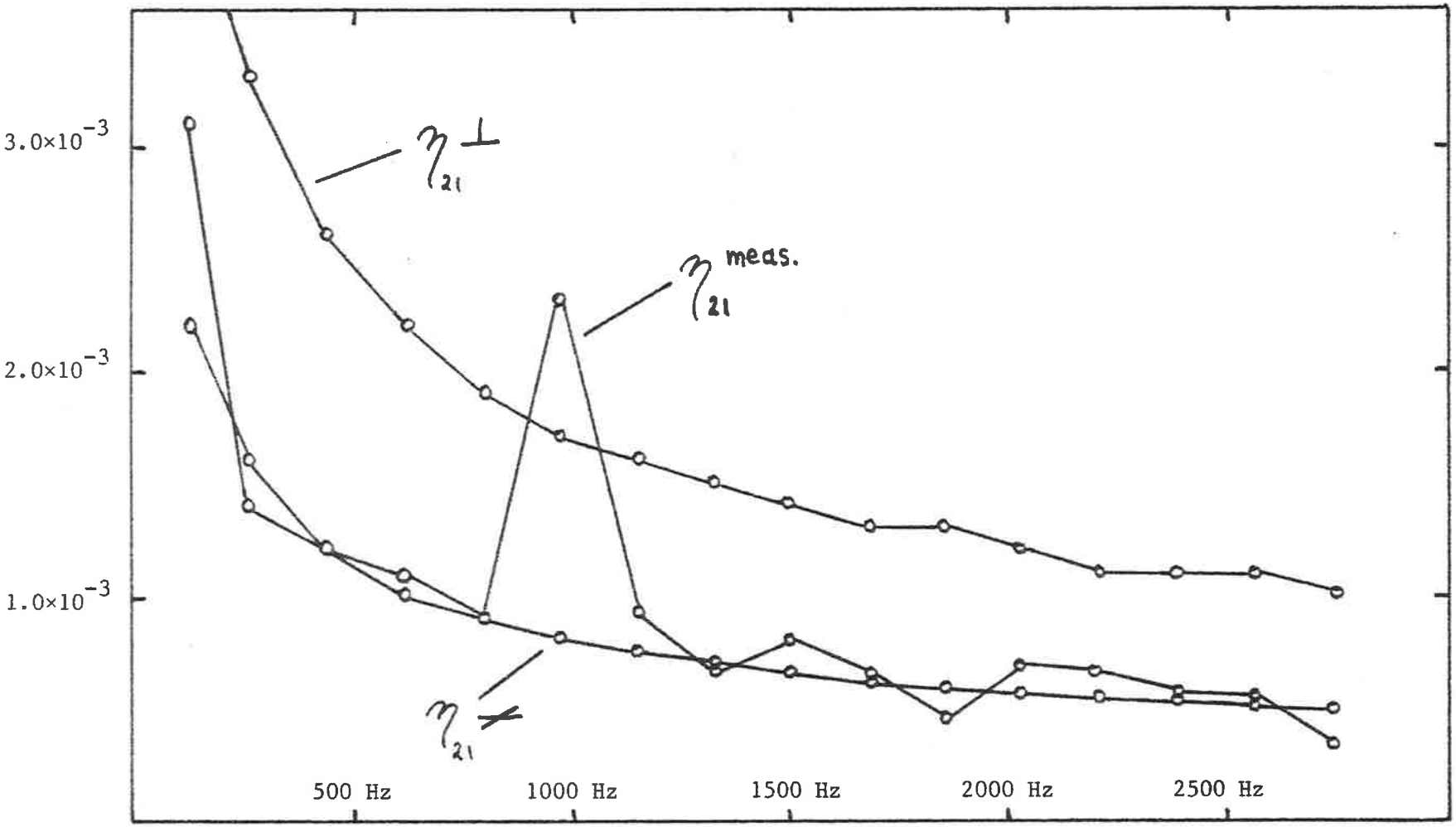

Fig. 6b Coupling loss factor measured 'in situ' and theoretical prediction for normal incidence and average oblique incidence

unexplained peak).

5.6. Flexural to Longitudinal Wave Transformation

The loss factors were deduced from energy balance equations which were based on the energy stored in the flexural modes of the test-structure. The energy stored in the longitudinal modes was neglected. The following considerations deal with the validity of this approximation.

Consider a flexural wave of unit energy, normally incident at the right angle corner between two plates. A fraction τ_{FF} of this unit energy incident wave is transmitted across the junction as a flexural wave, and similarly, a fraction ρ_{FF} is reflected. A fraction τ_{FL} of the unit energy incident wave is transmitted as a longitudinal wave, and similarly a fraction ρ_{FL} is reflected. Evidently,

$$\tau_{FF} + \rho_{FF} + \tau_{FL} + \rho_{FL} = 1 \quad .$$

Cremer and Heckl (Cremer and Heckl and Ungar, 1973 pp 316-334) have derived expressions to compute these transmission and reflection efficiencies. A computer program was written to evaluate these (rather complicated) expressions. The results are plotted on Figure 7, covering the five Octave bands of interest for the test-structure. As can be seen from Figure 7, longitudinal waves are only likely to play a significant role in the 2 kHz Octave band.

5.7. The Least Squares Method

The energy balance equations can be written in a general form

$$P^i = \sum_j \eta_j \, E^i_j$$

where η_j is the loss factor between subsystem j and i (i.e. a coupling loss factor when $j \neq i$, and internal loss factor when $j = i$), and E^i_j is the energy stored in subsystem j when P^i is injected into sub-

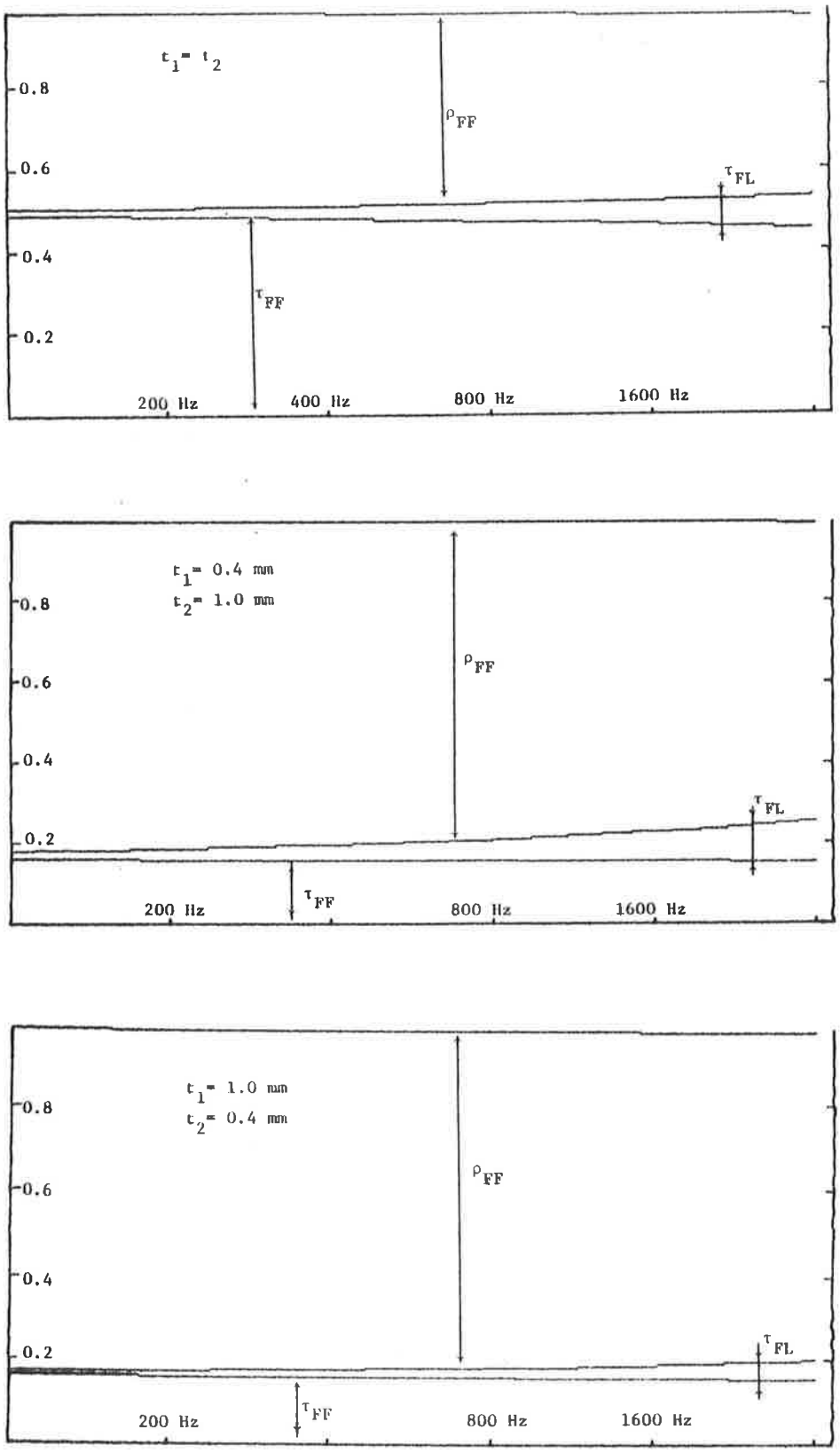

Fig. 7 Theoretical transmission efficiency and reflection efficiency across a corner junction. L stands for longitudinal, F for flexural.

system i.

Consider

$$\Delta^i = P^i - \sum_j \eta_j \, E_j^i \quad .$$

Applying the least squares principle yields the following k equations:

$$\frac{\partial}{\partial \eta_k} \left[\sum_i (\Delta^i)^2 \right] = 0$$

or

$$\sum_j \eta_j \left(\sum_i E_j^i \, E_k^i \right) = \sum_i P^i \, E_k^i \quad .$$

This symmetric system of k equations can be solved to find the k loss factors. A program was developed to construct such a system from the data recorded on the test structure. This was applied to the 500 Hz Octave band, taking 80 modes together. The resulting loss factors (Table 12) were not substantially different from those obtained previously (Table 8). Thus, the simpler procedure of averaging the results appears quite adequate.

...ooo000ooo...

TABLE 12

LEAST SQUARES FIT (500 Hz Octave Band)

$$\begin{bmatrix} 3.2 & 3.2 & -1.1 & 0.0 \\ 3.2 & 6.5 & -2.3 & -1.1 \\ -1.1 & -2.3 & 1.5 & 0.73 \\ 0.0 & -1.1 & 0.73 & 0.73 \end{bmatrix} \begin{bmatrix} 1.98 \\ 1.72 \\ 3.26 \\ 4.67 \end{bmatrix} = \begin{bmatrix} 8.2 \\ 4.8 \\ 2.0 \\ 3.9 \end{bmatrix}$$

$$\begin{bmatrix} 2.1 & 2.1 & -0.74 & 0.0 \\ 2.1 & 4.1 & -1.5 & -0.74 \\ -0.74 & -1.5 & 0.87 & 0.44 \\ 0.0 & -0.74 & 0.44 & 0.44 \end{bmatrix} \begin{bmatrix} 1.91 \\ 2.71 \\ 3.89 \\ 7.10 \end{bmatrix} = \begin{bmatrix} 6.7 \\ 4.2 \\ 1.1 \\ 2.8 \end{bmatrix}$$

Frequency [Hz]	η_{11} x 1000	η_{12} x 1000	η_{21} x 1000	η_{22} x 1000
442	0.71	0.62	1.2	1.7
619	0.49	0.70	1.0	1.8

N.B. The loss factors are the solutions to the above systems, divided by ω_c.

CONCLUSION

The Statistical Energy Analysis (SEA) loss factors of simple multi-modal structures can be determined 'in situ' by solving the energy balance equations of the SEA model. These energy balance equations result from spectral estimates of energies stored in, and powers injected into the various elements (i.e. groups of similar modes) of the model. It is therefore essential to include in the model all significant forms of vibrational energy, and to be able to measure accurately the corresponding stored energies and injected powers.

The loss factors are obtained indirectly from measured quantities, and experimental errors are therefore magnified by sensitivity coefficients greater than unity. In general each loss factor has a different sensitivity coefficient. Consequently, some loss factors can be determined more accurately than others. Also, the sensitivity coefficients depend on the actual loss factors. A detailed analysis of two coupled systems showed how the sensitivity coefficients compare with each other. In brief, the internal loss factors have larger sensitivity coefficients than the coupling loss factors.

The 'in situ' method was applied to a test-structure consisting of two thin steel plates welded at right angles to each other. The SEA model consisted of the flexural modes of each plate, i.e. two coupled multi-modal systems. In order to determine the stored energies and injected powers with good accuracy, a large number of measurements was found to be inevitable. As one would expect, a delicate aspect was the measurement of the injected power. Analogue techniques were found to be very tedious, inflexible and fairly inaccurate. Consequently, a digital system was designed to perform the experiment. This system lived up to expectations, and the test-structure was analysed over five Octave-bands by using a sizeable amount of data and computing time.

Possible improvements on the hardware as well as the software aspects were discussed in some detail. In the light of this discussion, it appeared that the 'in situ' method is limited to only a few coupled multi-modal systems. This is because the complexity of the method is directly proportional to the square of the number of systems. An upper limit of four coupled systems is suggested, but this is arguable. At any rate, it seems quite certain that the 'in situ' approach is not applicable to complex structures with say one hundred multi-modal systems e.g. a very large ship. However, such complex structures could perhaps be broken down into smaller structures, and these analysed separately.

The data collected on the test-structure was processed to provide some indication on the spread of the measured quantities around their mean. The stored energy (obtained from an average of eight transverse accelerations) was averaged over five driving points. A rather wide spread was observed for these five estimates. Consequently, the space-average of the various quantities could be further improved at the cost of an even larger amount of data - e.g. twelve transverse accelerations and ten driving points. An accurate time-average of the spectral quantities was found to require approximately one hundred uncorrelated estimates (N.B. depending on the desired frequency resolution). This number could be reduced by using more sophisticated algorithms and techniques.

The loss factors measured 'in situ' on the test-structure presented some interesting properties -- the detrimental effect of the sensitivity coefficients was clearly demonstrated -- the 'in situ' coupling loss factors and their theoretical predictions were in good agreement. In fact, excellent agreement was found between one coupling loss factor and the average-oblique-incidence wave-transmission prediction.

In summary, a digital system which implements the 'in situ' method has been developed and applied to a test-structure. Loss factors were determined successfully over five Octave-bands. The 'in situ' method was found to have two inherent drawbacks : a certain degree of inaccuracy and the necessity for very large numbers of measurements. However, when theoretical predictions are not available or cannot be fully trusted, this method is probably the best suited to provide all steady-state loss factors at once.

It is hoped that the techniques and results outlined in this thesis will provide useful information for future applications of Statistical Energy Analysis to engineering projects.

...oooOOOooo...

APPENDIX A

EQUIPMENT

Noise Source

The noise source used throughout this project was a Bruel & Kjaer Random Noise generator type 1402. The random noise was fed through an analogue Bruel & Kjaer Band-pass filter set type 1612. The resulting Octave-band white noise was then applied to a Bruel & Kjaer Mini-shaker type 4810.

Force-acceleration Transducer

The acceleration signal was supplied by a Bruel & Kjaer (B&K) miniature accelerometer type 4344 (serial number 378473), the force signal by a piezo-electric crystal under compression. Both the accelerometer and the crystal were mounted in a compact form as shown in Figure A1 which represents the force-acceleration transducer schematically.

The tensioning nut was adjusted to ensure linearity of the force signal. The force and acceleration signals remained in phase when driving the transducer without load or with a mass-load at frequencies ranging from 80 Hz to 3 kHz. This proved the internal loss of the transducer to be negligible for all practical purposes.

Calibration was performed by measuring the force/acceleration ratio at the five Octave-band centre frequencies for a range of mass-loads (see Table A1). For each frequency, a linear regression line was fitted through the experimental data. These five equations were then averaged. The voltage sensitivity of the transducer's accelerometer being known, the force calibration constant was easily deduced. These steps are shown in Table A2.

The driven side and the driving side of the transducer were bolted respectively to the B&K mini-shaker and the test-structure.

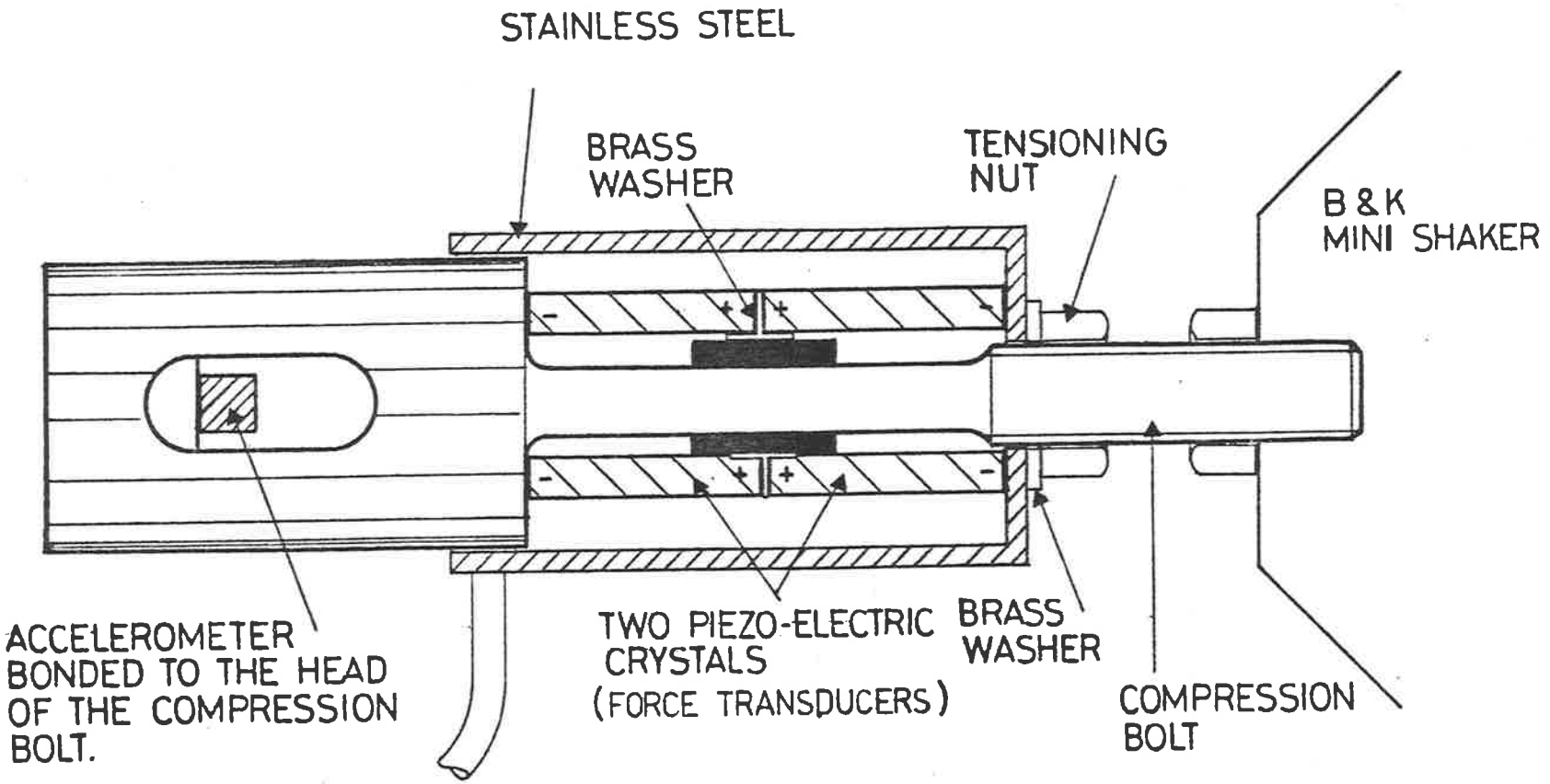

Fig. A1 Force-acceleration transducer

TABLE A1

f[Hz]	f/a no load	f/a 14 gr load	f/a 27 gr load	f/a 47.2 gr load
125	66.6	97.2	121.3	171.3
250	57.7	83.9	108.3	145.3
500	60.0	86.7	110.8	148.9
1000	60.5	87.9	113.5	165.3
2000	58.9	85.2	110.6	146.4

TABLE A2

f[Hz]	Linear Regression	Correlation Coefficient
125	f/a = 2.20 x m[gr] + 65.6	0.99840
250	f/a = 1.86 x m[gr] + 57.9	0.99998
500	f/a = 1.88 x m[gr] + 60.1	0.99999
1000	f/a = 2.22 x m[gr] + 57.9	0.99718
2000	f/a = 1.86 x m[gr] + 59.3	0.99978

Average Equation: f/a = 2.00 x m[gr] + 60.2

Acceleration Calibration Constant: 0.304 mV/ms^{-2} or 3.29 $m.s^{-2}/mV$ for accelerometer #378473

Force Calibration Constant: 0.304 x 2.00 = 0.610 V/N or 1.64 N/V for piezo-electric crystal

Accelerometers

The mean-square acceleration of each plate was obtained by averaging several (eight) point accelerations. These point accelerations were supplied by B&K miniature accelerometers type 4344, bolted to the plates. The frequency response of these accelerometers widely covers the five Octave-bands of interest (centred from 125 Hz to 2 kHz). Each accelerometer weighed about 2.7 gr and in view of the plates' thicknesses correction for mass-loading was applied according to the following formula :

$$a_{actual} = a_{measured} \times \frac{Z + j\omega m}{Z}$$

where ω is the angular frequency, m the mass of the accelerometer and Z the space- and frequency-average point-input impedance (Beranek, 1971).

Only the original cables were connected to the accelerometers, hence no correction for cable capacitance was needed and the factory calibration constants were applicable, as shown in Table A3.

Amplifiers

Ten pre-amplifiers and ten amplifiers were specially built to be able to measure the signals issued by the nine B&K 4344 accelerometers and by the piezo-electric force sensor. These amplifiers were calibrated to within 2% relative error over the frequency range of interest - i.e. 80 Hz to 3 kHz.

Analogue/Digital Converter

A 10-channel 8-bit A/D converter was used to digitize the signals sensed on the test structure. The -5V to +5V range was covered by linearly spaced integers ranging from -128 to +127.

TABLE A3

CALIBRATION CONSTANTS FOR BRUEL & KJAER ACCELEROMETERS TYPE 4344

Serial # 820 473	0.324 mV/m.s^{-2}	3.78 m.s^{-2}/mV
Serial # 820 477	0.261 mV/m.s^{-2}	4.66 m.s^{-2}/mV
Serial # 820 478	0.287 mV/m.s^{-2}	4.24 m.s^{-2}/mV
Serial # 820 479	0.269 mV/m.s^{-2}	4.52 m.s^{-2}/mV
Serial # 820 480	0.320 mV/m.s^{-2}	3.85 m.s^{-2}/mV
Serial # 820 481	0.312 mV/m.s^{-2}	3.92 m.s^{-2}/mV
Serial # 820 482	0.299 mV/m.s^{-2}	4.09 m.s^{-2}/mV
Serial # 820 484	0.292 mV/m.s^{-2}	4.20 m.s^{-2}/mV

A characteristic of random noise is the presence of spikes and sudden surges in amplitude. This meant that on average only six to seven bits were significant in order to avoid truncating these spikes and surges.

A systematic error on the injected power resulted at high frequencies because of the A/D converter's operating mode. Given a sampling rate f_s [Hz], a 'start conversion' signal was issued by a clock every $\frac{1}{f_s}$ [s]. Upon receipt of this signal, the converter would sample the ten channels sequentially at 6.2 μs intervals, then transfer the results to computer memory, and then wait for the next clock signal. The force and acceleration signals issued by the transducer were always connected to the first and second channel respectively, which meant a lag of 6.2 μs between these two signals. The relative error E introduced on the average product of the force F and the velocity V (time integration of the acceleration) can be estimated as follows,

$$E = \left| \frac{\frac{FV}{2} \cos(\phi + 2\pi f.\Delta t) - \frac{FV}{2} \cos\phi}{\frac{FV}{2} \cos\phi} \right|$$

where ϕ is the actual phase, f the frequency and Δt the time lag. Thus,

$$E = \left| \cos(2\pi f.\Delta t) - tg(\phi) \times \sin(2\pi f.\Delta t) - 1 \right|$$

and with $2\pi f.\Delta t < 2\pi \times 3000 \times 6.2 \times 10^{-6} = 0.1169$

$$E < 0.0068 + tg(\phi) \times 0.1166 \simeq 0.12 \times tg\,\phi \ .$$

In conclusion, the error is likely to be significant at high frequencies (i.e. in the 2 kHz Octave-band) if ϕ is close to 90° (which corresponds to zero injected power).

...ooo000ooo...

APPENDIX B

COMPUTER PROGRAMS

Programs which performed general purpose tasks are not presented here - e.g. standard deviation, plotting, averaging, solving a linear system of algebraic equations etc. Programs which performed specialised operations are also omitted - e.g. data unpacking, data transfer to and from magnetic tapes, least-squares fit to the data as an alternate way to construct the energy balance equations etc. It was thought that only three computer programs should be described here: the sampling program, the processing program and a program to compute a linear prediction filter.

The sampling program was used to collect the data from the test-structure. As such it shows how the 'in situ' experiment was actually performed. The processing program was responsible for most of the 'number crunching'. This was where calibration constants, experimental data, Fast Fourier Transform etc., all came together. The linear prediction filter program was used to compute the Maximum Entropy PSD. As one of the most obvious and promising improvements discussed in Section 4.5, it is not felt out of place here.

The structure of a well-written PASCAL program immediately tells how the problem is solved. The 'identifiers (i.e. the names of variables, procedures, types etc.) speak for themselves. Also the structured variables designed by the programmer indicate what tools are used. For example -- constant memory = 20480 -- variable core : array [1.. memory] of integer -- procedure fillcore(core). To study a PASCAL procedure

(a program is also a procedure), one starts with the 'heading' which contains the variables, types and constants defined within that procedure. Next one takes the 'body' which is the sequence of operations performed by the procedure. Each of the following three programs should be examined according to this method.

Program 'sample'

Program 'sample' collects binary data from an A/D converter and stores it in file 'data' on a floppy disk. Since the data cannot always fit on a single disk, the program interrupts after filling one disk with a large file, waiting for a new mass storage volume to be inserted. Data relevant to the experiment, such as amplifier gain, sampling rate etc. is appended to each file. Note that each 8-bit sample is stored in one half 16-bit word.

Procedure 'tune' issues an audible signal when a new mass storage volume is required. Procedure 'arget' is the machine language external procedure which drives the A/D converter. Procedure 'nextname' increments the file name attribute by one when the current mass storage volume is full - e.g. "MYDATA.104" becomes "MYDATA.105". Note that it is up to the experimenter to make sure that the number of data records (i.e. 'numinlot') will fit on a single mass storage volume.

Program 'process'

Program 'process' computes the injected power and the 8-point stored energy. The input file 'data' contains 'numinlot' time records (see Section 4.4). The external file 'sys' contains the physical characteristics of the test-structure. After computation, the output files 'pow' and 'energ' contain 'numinlot' injected powers and 8-point stored energies respectively.

Procedure 'getready' computes various quantities such as amplifier gains, point-input impedance, frequency seperation etc. needed by the program. Procedure 'init' computes the Kaiser-Bessel window, using the external function MMBSIO which returns the I_o Bessel function. 'inpower' inputs the transducer's force and acceleration data. 'FFT2C' is an external function which performs a Fast Fourier Transform according to the following formula :

$$X_p = \sum_{k=0}^{N-1} x_k \cdot e^{2\pi j \frac{pk}{N}} \qquad p = 0,1.. N-1 \quad (j = \sqrt{-1}\ ).$$

'outpower' finds the average injected power (see Section 4.3.3). 'scpow' scales the injected power according to the calibration constants, amplifier gains and A/D converter sensitivity. 'inpsd' inputs the transverse acceleration data. 'outpsd' finds the power spectrum of the transverse acceleration (see Section 4.3.2). 'acengy' scales the power spectrum of the transverse acceleration to obtain the point energy stored in the plate according to calibration constants, amplifier gains, A/D converter sensitivity and mass-loading correction.

Program 'linpred'

Program 'linpred' finds a Linear Prediction filter which fits the time series contained in file 'data'. The filter coefficients a_k k= 1,2.. 'order' and the error power 'pow' are output on file 'fil'. The computations proceed according to Andersen's flowchart (Andersen, 1974). The order of the filter (i.e. the number of coefficients) is determined by the Final Prediction-error criterion (FPE) as given by Haykin (Haykin, 1979).

Given a time series x_n n = 1,2.. N, a linear prediction filter of order m has the following properties:

$$x_n \simeq \tilde{x}_{n,f} = a_1 x_{n-1} + a_2 x_{n-2} + \ldots + a_m x_{n-m} = \sum_{k=1}^{m} a_k x_{n-k}$$

$$n = m+1,\ m+2,\ ..N \qquad \text{(forward operation)}$$

$$x_n \simeq \tilde{x}_{n,b} = a_1 x_{n+1} + a_2 x_{n+2} + \ldots + a_m x_{n+m} = \sum_{k=1}^{m} a_k x_{n+k}$$

$$n = 1,2..\ N-m \qquad \text{(backward operation)}$$

where the filter coefficients a_k k=1,2 ..m are chosen in order to minimize the forward and backward error powers P_f and P_b given by

$$P_f = \sum_{n=m+1}^{N} e_{n,f}^2 = \sum_{n=m+1}^{N} (\tilde{x}_{n,f} - x_n)^2$$

$$P_b = \sum_{n=1}^{N-m} e_{n,b}^2 = \sum_{n=1}^{N-m} (\tilde{x}_{n,b} - x_n)^2.$$

The Maximum Entropy Power Spectral Density PSDMEM of the time series x_n n = 1,2 .. N is then given by (Haykin, 1979) :

$$\text{PSDMEM}(f) = \frac{\text{'pow'}/f_s}{\left| 1 - \sum_{k=1}^{\text{'order'}} a_k e^{-2\pi j \frac{kf}{f_s}} \right|^2}$$

where f is the frequency, 'pow' is the error power as computed by program 'linpred', f_s is the sampling rate of x_n, a_k k= 1,2.. 'order' are the linear prediction filter coefficients as computed by 'linpred' and j is $\sqrt{-1}$.

```
program sample ;

const
  namelen = 15 ;
  wordnum = 5 ;
  memory = 20480 ;
  field = 6 ;

var
  data : file of integer ;
  core : array[1..memory] of integer ;
  name : array[0..namelen] of char ;
  dot : 0..namelen ;
  samples,channels,words,totalwords : integer ;
  gain,samplrate,count : integer ;
  gains : array[1..10] of integer ;
  wordcount,samplecount : integer ;
  numoflots,numinlot : integer ;
  lotcount,recordcount : integer ;
  ch : char ;

procedure ask ;

begin {ask}
writeln ; writeln ;
write('sampling rate ?') ;
break(output) ; readln(samplrate) ;
write('how many samples ?') ;
break(output) ; readln(samples) ;
write('how many channels ?') ;
break(output) ; readln(channels) ;
writeln ;
for count := 1 to channels do begin
  write('dB gain for channel ',count:2,' :') ;
  break(output) ; readln(gain) ;
  gains[count] := gain ;
end ;
writeln ;
write('# of data files ?') ;
break(output) ; readln(numoflots) ;
write('# of records in 1 data file ?') ;
break(output) ; readln(numinlot) ;
end {ask} ;

procedure display ;

begin {display}
writeln ; writeln ;
writeln('sampling rate ---------------- :',samplrate:field) ;
writeln('# of samples ----------------- :',samples : field) ;
for count := 1 to channels do begin
  writeln('gain for channel ',count:2,' ----------- :',gains[count]:field) ;
end ;
writeln('# of data files -------------- :',numoflots:field) ;
writeln('# of records in 1 data file --- :',numinlot:field) ;
writeln ;
write('first data file name is :') ;
count := 0 ;
```

```
repeat
  write(argv[2]↑[count]) ;
  count := succ(count) ;
until argv[2]↑[count] = chr(0) ;
end {display} ;

procedure nextname ;

begin {nextname}
count := 0 ;
repeat count := succ(count) until argv[2]↑[count] = '.' ;
if argv[2]↑[count+3] <> '9' then begin
  argv[2]↑[count+3] := succ(argv[2]↑[count+3] ;
end else begin
  argv[2]↑[count+3] := '0' '
  if argv[2]↑[count+2] <> '9' then begin
    argv[2]↑[count+2] := succ(argv[2]↑[count+2] ;
  end else begin
    argv[2]↑[count+2] := '0' ;
    argv[2]↑[count+1] := succ(argv[2]↑[count+1] ;
  end ;
end ;
end {nextname} ;

procedure arget(var samples : integer ;
                var core : array[1..memory] of integer ;
                var totalwords : integer) ; fortran ;

procedure tune ;

var
  count : integer ;

procedure pause(t : integer) ;

const
  a = 1.0 ;

var
  re : real ;
  cl : integer ;

begin {pause}
for cl := 1 to t do begin
  re := a/a*a/a*a/a*a/a*a/a*a ;
end ;
end {pause} ;

procedure ring ;

const
  bell = chr(7) ;

begin {ring}
write(bell) ;
break(output) ;
end {ring} ;
```

```
begin {tune}
count := 0 ;
repeat
  count := succ(count) ;
  pause(10000) ; ring ;
  pause(2500) ; ring ;
  pause(2500) ; ring ;
  pause(1500) ; ring ;
  pause(1500) ; ring ;
  pause(2800) ; ring ;
  pause(1500) ; ring ;
  pause(1500) ; ring ;
  pause(1500) ; ring ;
  pause(2500) ; ring ;
  pause(1500) ; ring ;
until count = 3 ;
end {tune} ;

procedure doit ;

begin {doit}
dot := 0 ;
repeat dot := succ(dot) until argv[2]↑[dot] = '.' ;
for lotcount := 1 to numoflots do begin
  writeln ; writeln ;
  write('insert new volume !!!') ;
  break(output) ; tune ; readln(ch) ;
  rewrite(data,argv[2]↑) ;
  data↑ := samplrate ; put(data) ;
  data↑ := samples ; put(data) ;
  data↑ := channels ; put(data) ;
  for count := 1 to channels do begin
    data↑ := gains[count] ; put(data) ;
  end ;
  data↑ := numinlot ; put(data) ;
  for recordcount := 1 to numinlot do begin
    arget(samples,core,totalwords) ;
    for wordcount := 1 to words do begin
      for samplecount := 0 to samples-1 do begin
        data↑ := core[samplecount * wordnum + wordcount] ; put(data) ;
      end ;
    end ;
    writeln('record ',recordcount:1,' in data file ',lotcount:1) ;
    break(output) ;
  end ;
  for count := 0 to namelen do name[count] := argv[2]↑[count] ;
  name[dot+4] := chr(0) ;
  reset(data,name) ;
  nextname ;
end ;
end  {doit} ;

begin {main}
ask ;
words := channels div 2 + channels mod 2 ;
totalwords := samples * wordnum ;
display ;
writeln ; writeln ;
write('all OK ?') ;
break(output) ; readln(ch) ;
```

```
if ch = 'Y' then begin
  doit ;
end else begin
  writeln ; writeln ;
  writeln('Wrong entry. Try again !!!') ;
end ;
end.
```

N.B. Program 'sample' was written for the NBS-Pascal compiler. As such it presents some 'non-standard' features :-

a) external file variables can be omitted from the program declaration

b) external file names are found in an array of pointers called 'argv'

c) function 'break(filevariable)' empties the file buffer

d) structured constants are allowed

e) procedure and function declarations allow a type declaration instead of an identifier

etc.

```
program process(data,pow,energ,sys,input,output) ;

const
  bitunit = 0.0390625 ;  {V/bit}
  transaccel = 3290.0 ;  {m.s^-2/V}
  transforc = 1.64 ;  {N/V}
  accelmass = 2.7 ;  {gr}
  pi = 3.14159 ;
  acc1 = 3.78 ;  {m.s^-2/mV}
  acc2 = 4.66 ;
  acc3 = 4.24 ;
  acc4 = 4.52 ;
  acc5 = 3.85 ;
  acc6 = 3.92 ;
  acc7 = 4.09 ;
  acc8 = 4.20 ;
  kaiserparam = 3.0 ;
  maxrecord = 4096 ;
  windowlen = 2048 ; {maxrecord/2}
  maxpowtwo = 12 ; {power of two of maxrecord}

type
  plate = record
            last : boolean ;
            mass : real ;  {kg}
            area : real ;  {m^2}
            thick : real ;  {mm}
            dens : real ;  {kg/m^3}
            speed : real    {m/s}
          end ;
  complex = (rel,imag) ;
  workvector = array[1..maxrecord] of array[rel..imag] of real ;
  scrapvector = array[0..maxpowtwo] of integer ;
  windowtype = array[0..windowlen] of real ;
  buffer = array[1..windowlen] of real ;
  blokfile = segmented file of real ;

var
  xx : workvector ;
  iwk : scrapvector ;
  windpow,windener : windowtype ;
  samples,samplediv2,samplediv4,srate,channels,numinlot,powtwo : integer ;
  parseval,parseval1,parseval2 : real ;
  impedance,scale,temp1,temp2,fqunit : real ;
  gains : array[1..10] of real ;
  thisplate : plate ;
  system : integer ;
  sys : file of plate ;
  data : file of integer ;
  outbuf,averag : buffer ;
  pow,energ : blokfile ;
  cntrec,cnt : integer ;

function findgain(dB : integer) : real ;

const
  shift = 5 ; {Ian's design} ;

var
  temp : real ;
```

```
begin {findgain}
temp := (dB - shift) / 20.0 ;
findgain := exp(temp * ln(10)) ;
end {fingain} ;

procedure getready ;

var
  count : integer ;

begin {getready}
writeln('which system?') ;
read(system) ;
for count := 1 to system-1 do get(sys) ;
thisplate := sys↑ ;
srate := data↑ ; get(data) ;
samples := data↑ ; get(data) ;
channels := data↑ ; get(data) ;
for count := 1 to channels do begin
  gains[count] := findgain(data↑) ;
  get(data) ;
end ;
numinlot := data↑ ; get(data) ;
powtwo := 0 ;
samplediv2 := samples ;
repeat
  samplediv2 := samplediv2 div 2 ;
  powtwo := succ(powtwo) ;
until samplediv2 = 1 ;
samplediv2 := samples div 2 ;
samplediv4 := samples div 4 ;
scale := sqr(bitunit) * transaccel * transforc / gains[1] / gains[2] ;
impedance := thisplate.dens * thisplate.speed
                            * sqr(thisplate.thick * 0.001) ;
impedance := impedance * 4.0 / sqrt(3) ;
temp1 := 2.0 * pi * accelmass * 0.001 / impedance ;
temp2 := sqr(bitunit) * thisplate.mass / 2.0 / pi ;
fqunit := srate / samples ;
end {getready} ;

procedure init(length : integer ; var window : windowtype) ;

var
  tableentry,tableinterval,temp1,temp2,param : real ;
  count : integer ;
  iopt,ier : integer ; {parameters for Bessel function}

function MMBSI0(var iopt : integer ;
                var arg : real ;
                var ier : integer) : real ; fortran ;

begin {init}
param := kaiserparam * pi ;
iopt := 1 ;
temp1 := MMBSI0(iopt,param,ier) ;
tableentry := 0.0 ;
tableinterval := pi / length ;
```

```
for count := 0 to length do begin
  temp2 := param * sqrt(1.0 - sqr(count / length - 1.0)) ;
  window[count] := MMBSIO(iopt,temp2,ier) / temp1 ;
  tableentry := tableentry + tableinterval ;
end ;
end {init} ;

procedure inpower(var xx : workvector ; var window : windowtype) ;

var
  num1,num2,denom1,denom2 : real ;
  count : integer ;
  realpart,imagpart,temp : real ;

begin {inpower}
num1 := 0.0 ; num2 := 0.0 ;
denom1 := 0.0 ; denom2 := 0.0 ;
for count := 1 to samples do begin
  if count-1 <= samplediv2 then temp := window[count-1]
                           else temp := window[samples-count+1] ;
  realpart := data↑ ; get(data) ;
  num1 := num1 + sqr(realpart) ;
  realpart := realpart * temp ;
  xx[count,rel] := realpart ;
  denom1 := denom1 + sqr(realpart) ;
end ;
for count := 1 to samples do begin
  if count-1 <= samplediv2 then temp := window[count-1]
                           else temp := window[samples-count+1] ;
  imagpart := -data↑ ; get(data) ;
  num2 := num2 + sqr(imagpart) ;
  imagpart := imagpart * temp ;
  xx[count,imag] := imagpart ;
  denom2 := denom2 + sqr(imagpart) ;
end ;
parseval1 := num1 / denom1 ;
parseval2 := num2 / denom2 ;
end {inpower} ;

procedure outpower(var xx : workvector ; var out : buffer) ;

var
  count,shift : integer ;
  real1,real2,imag1,imag2 : real ;
  freq,incr : real ;

begin {outpower}
parseval1 := parseval1 / sqr(samples) ;
parseval2 := parseval2 / sqr(samples) ;
parseval := 0.5 * sqrt(parseval1 * parseval2) ;
out[1] := 0.0 ; {no DC allowed}
incr := srate * 2.0 * pi / samples ;
freq := 0.0 ;
for count := 2 to samplediv2 do begin
  freq := freq + incr ;
  shift := samples + 2 - count ;
```

```
  real1 := xx[count,rel] ; real2 := xx[shift,rel] ;
  imag1 := xx[count,imag] ; imag2 := xx[shift,imag] ;
  out[count] := abs(parseval / freq
             * (-sqr(real1) + sqr(real2) - sqr(imag1) + sqr(imag2))) ;
end ;
end {outpower} ;

procedure scpow(var out : buffer) ;

var
  count : integer ;

begin {scpow}
for count := 1 to samplediv2 do out[count] := out[count] * scale ;
end {scpow} ;

procedure zero(var av : buffer) ;

var
  count : integer ;

begin {zero}
for count := 1 to samplediv2 do av[count] := 0.0 ;
end {zero} ;

procedure inpsd(var xx : workvector ; var window : windowtype) ;

var
  num,denom : real ;
  count : integer ;
  realpart,imagpart,temp : real ;

begin {inpsd}
num := 0.0 ; denom := 0.0 ;
for count := 1 to samplediv2 do begin
  if count <= samplediv4 then temp := window[count-1]
                         else temp := window[samplediv2-count+1] ;
  realpart := data↑ ; get(data) ;
  imagpart := -data↑ ; get(data) ;
  num := num + sqr(realpart) + sqr(imagpart) ;
  realpart := realpart * temp ;
  imagpart := imagpart * temp ;
  xx[count,rel] := realpart ;
  xx[count,imag] := imagpart ;
  denom := denom + sqr(realpart) + sqr(imagpart) ;
end ;
parseval := num / denom ;
end {inpsd} ;

procedure outpsd(var xx : workvector ; var out : buffer) ;

var
  count,shift : integer ;
  real1,real2,imag1,imag2,sine,cosine : real ;
  arg,incr,realpart,imagpart : real ;
```

```
begin {outpsd}
parseval := parseval / sqr(samples) ;
realpart := xx[1,rel] + xx[1,imag] ;
imagpart := 0.0 ;
out[1] := parseval * (sqr(realpart) + sqr(imagpart)) ;
incr := pi / samplediv2 ;
arg := 0.0 ;
parseval := parseval / 2.0 ;
for count := 2 to samplediv2 do begin
  arg := arg + incr ;
  shift := samplediv2 + 2 - count ;
  real1 := xx[count,rel] ; real2 := xx[shift,rel] ;
  imag1 := -xx[count,imag] ; imag2 := -xx[shift,imag] ;
  cosine := cos(arg) ; sine := sin(arg) ;
  realpart := real1 + real2 + cosine * (imag1 + imag2)
                            -   sine * (real1 - real2) ;
  imagpart := imag1 - imag2 -   sine * (imag1 + imag2)
                            - cosine * (real1 - real2) ;
  out[count] := parseval * (sqr(realpart) + sqr(imagpart)) ;
end ;
end {outpsd} ;

procedure acengy(accel : integer ; var out : buffer) ;

var
  sensitivity,massloading,freq,temp : real ;
  count : integer ;

procedure select(number : integer ; var sens : real) ;

begin {select}
case number of
  1 : sens := acc1 ;
  2 : sens := acc2 ;
  3 : sens := acc3 ;
  4 : sens := acc4 ;
  5 : sens := acc5 ;
  6 : sens := acc6 ;
  7 : sens := acc7 ;
  8 : sens := acc8
end ;
sens := sens * 1000.0 ;
end {select} ;

begin {acengy}
select(accel,sensitivity) ;
out[1] := 0.0 ;
freq := 0.0 ;
temp := temp2 * sqr(sensitivity / gains[accel+2]) ;
for count := 2 to samplediv2 do begin
  freq := freq + fqunit ;
  massloading := 1.0 + sqr(temp1 * freq) ;
  out[count] := out[count] * temp * massloading / sqr(freq) ;
end ;
end {acengy} ;
```

```
procedure add(var out,av : buffer) ;

var
  count : integer ;

begin {add}
for count := 1 to samplediv2 do av[count] := av[count] + out[count] ;
end {add} ;

procedure divide(var av : buffer) ;

var
  count : integer ;

begin {divide}
for count := 1 to samplediv2 do av[count] := av[count] / 8.0 ;
end {divide} ;

procedure copy(var buf : buffer ; var fil : blokfile) ;

var
  count : integer ;

begin {copy}
for count := 1 to samplediv2 do begin
  fil↑ := buf[count] ;
  put(fil) ;
end ;
putseg(fil) ;
end {copy} ;

procedure FFT2C(var a : workvector ;
                var m : integer ;
                var iwk : scrapvector) ; fortran ;

begin {main}
reset(data) ; rewrite(pow) ; rewrite(energ) ; reset(sys) ;
getready ;
init(samplediv2,windpow) ;
init(samplediv4,windener) ;
for cntrec := 1 to numinlot do begin
  inpower(xx,windpow) ;
  FFT2C(xx,powtwo,iwk) ;
  outpower(xx,outbuf) ;
  scpow(outbuf) ;
  copy(outbuf,pow) ;
  powtwo := pred(powtwo) ;
  zero(averag) ;
  for cnt := 1 to 8 do begin
    inpsd(xx,windener) ;
    FFT2C(xx,powtwo,iwk) ;
    outpsd(xx,outbuf) ;
    acengy(cnt,outbuf) ;
    add(outbuf,averag) ;
  end ;
  powtwo := succ(powtwo) ;
  divide(averag) ;
  copy(averag,energ) ;
  writeln('done record ',cntrec:1) ;
end ;
end.
```

```
program linpred(data,fil,output) ;

const
  samplemax = 4096 ;
  ordermax = 100 ;

var
  data : file of integer ;
  fil : file of real ;
  coeff,oldcoeff : array[1..ordermax] of real ;
  forw,backw : array[1..samplemax] of real ;
  order,count,samplenum : integer ;
  pow : real ;

procedure filter ;

var
  fpe,oldfpe : real ;
  exitout : boolean ;

procedure initialize ;

var
  cnt : integer ;

begin {initialize}
pow := 0.0 ;
samplenum := 0 ;
while not eof(data) do begin
  samplenum := succ(samplenum) ;
  forw[samplenum] := data↑ ; get(data) ;
  pow := pow + sqr(forw[samplenum]) ;
end ;
pow := pow / samplenum ;
for cnt := 2 to samplenum do begin
  backw[cnt-1] := forw[cnt] ;
end ;
order := 1 ;
fpe := pow * (samplenum + order + 1) / (samplenum - order - 1) ;
end {initialize} ;

procedure power ;

var
  num,denom : real ;
  cnt : integer ;

begin {power}
num := 0.0 ; denom := 0.0 ;
for cnt := 1 to samplenum-order do begin
  num := num + forw[cnt] * backw[cnt] ;
  denom := denom + sqr(forw[cnt]) + sqr(backw[cnt]) ;
end ;
coeff[order] := 2.0 * num / denom ;
pow := pow * (1.0 - sqr(coeff[order])) ;
oldfpe := fpe ;
fpe := pow * (samplenum + order + 1) / (samplenum - order - 1) ;
end {power} ;
```

```
procedure error ;

var
  cnt : integer ;

begin {error}
for cnt := 1 to order-1 do oldcoeff[cnt] := coeff[cnt] ;
for cnt := 1 to samplenum-order do begin
  forw[cnt] := forw[cnt] - backw[cnt] * coeff[order-1] ;
  backw[cnt] := backw[cnt+1] - forw[cnt+1] * coeff[order-1] ;
end ;
end {error} ;

procedure coefficients ;

var
  cnt : integer ;

begin {coefficients}
for cnt := 1 to order-1 do begin
  coeff[cnt] := oldcoeff[cnt] - oldcoeff[order-cnt] * coeff[order] ;
end ;
end {coefficients} ;

begin {filter}
initialize ;
power ;
exitout := false ;
repeat
  order :=  order + 1 ;
  error ;
  power ;
  coefficients ;
  if fpe > oldfpe then exitout := true ;
until exitout ;
end {filter} ;

begin {main}
reset(data) ;
filter ;
rewrite(fil) ;
fil↑ := samplenum ; put(fil) ;
fil↑ := order ; put(fil) ;
fil↑ := pow ; put(fil) ;
for count := 1 to order do begin
  fil↑ := coeff[count] ;
  put(fil) ;
end ;
end.
```

...ooo000ooo...

APPENDIX C

STATISTICAL ENERGY ANALYSIS OF COUPLED MULTI-MODAL STRUCTURES

An attempt is made here to study analytically two linearly coupled multi-modal structures. The steady-state modal responses to pure-tone excitation are solutions to a system of linear algebraic equations. This system can be solved analytically in two simple cases :- firstly when only few modes are involved e.g. a one-mode system coupled to a two-mode system; secondly when the inter-modal couplings and the modal forces are equal. The first case is fairly obvious since it amounts to solving a small linear system of equation. The second is non-trivial since a n+m by n+m system has to be solved (n and m are the number of modes in each system). The solution of this second case is presented here in detail.

The actual Statistical Energy Analysis equations are obtained by integrating over the frequency variable the sums of modal response complex products which correspond to average stored energies, average transmitted energies and average dissipated energies. In the simplest case (i.e. one mode coupled to one mode), the algebra is heavy, but manageable (Lyon, 1975). The second simplest case however (i.e. one mode coupled to two modes), very quickly produces some formidable algebra, and the case of identical couplings and identical modal forces likewise. Consequently, the analytical calculations were not pursued any further, and only the general procedure is outlined here. It is believed that a computer simulation of these equations would yield some interesting results. This however, was judged to be well beyond the scope of this project.

Consider two linearly coupled systems α and β. Under fairly general assumptions (Lyon, 1975), the steady-state modal amplitudes $X_{\alpha k}$ and $X_{\beta \ell}$ to a pure-tone excitation at angular frequency ω satisfy the following system of equations (the subscripts α and β refer to system α and β respectively, $i = \sqrt{-1}$):

$$M_\alpha \left[(\omega_{\alpha k}^2 - \omega^2) + i\omega\delta_{\alpha k} \right] X_{\alpha k} = F_{\alpha k} - \sum_{j=1}^{m} \left[(\kappa_{\beta\alpha jk} - \omega^2 \sigma_{\beta\alpha jk}) + i\omega\gamma_{\beta\alpha jk} \right] X_{\beta j}$$

$$k = 1,2.. \; n \qquad \text{[C1]}$$

$$M_\beta \left[(\omega_{\beta \ell}^2 - \omega^2) + i\omega\delta_{\beta \ell} \right] X_{\beta \ell} = F_{\beta \ell} - \sum_{j=1}^{n} \left[(\kappa_{\alpha\beta j\ell} - \omega^2 \sigma_{\alpha\beta j\ell}) + i\omega\gamma_{\alpha\beta j\ell} \right] X_{\alpha j}$$

$$\ell = 1,2.. \; m$$

System α of total mas M_α has n modes with resonance frequencies $\omega_{\alpha k}$ and internal dampings $\delta_{\alpha k}$. System β of mass M_β has m modes at $\omega_{\beta \ell}$ with damping $\delta_{\beta \ell}$. κ is an elastic force coefficient, σ an inertial force coefficient and γ a gyroscopic force coefficient. The subscripts of these force coefficients read as follows: $\kappa_{\beta\alpha jk}$ is the elastic force coefficent from mode j of system β to mode k of system α. $F_{\alpha k}$ is the amplitude of a modal excitation force.

It is important to bear in mind the physical meaning of these modal quantities. Using the mode shapes $\psi_{\alpha k}$ (r) k = 1,2.. n and $\psi_{\beta \ell}$ (r) ℓ = 1,2..m(which satisfy the boundary conditions plus the usual orthogonality relationships) where r stands for the space coordinates, the coupling coefficients are given by

$$\kappa_{\alpha\beta k\ell} = \int_{\text{junction}} ECS_{\alpha\beta}(r).\ \psi_{\alpha k}(r).\ \psi_{\beta\ell}(r).\ dr$$

$$\kappa_{\beta\alpha\ell k} = \int_{\text{junction}} ECS_{\beta\alpha}(r).\ \psi_{\alpha k}(r).\ \psi_{\beta\ell}(r).\ dr$$

where $ECS_{\alpha\beta}(r)$ is the elastic coupling strength between α and β (N.B. the junction between α and β is implicity defined as the region of space where $ECS_{\alpha\beta}(r) \neq 0$). Similar expressions can be written for the σ and γ coefficients. Also, the modal forces $F_{\alpha k}$ satisfy

$$F_{\alpha k}(t) = \int_{\alpha} f_{\alpha}(r,t).\ \psi_{\alpha k}(r).\ dr$$

where $f_{\alpha}(r,t)$ is the external force acting on system α, with

$$F_{\alpha k}(t) = F_{\alpha k} .\ e^{i\omega t}$$

in the case of pure-tone excitation at angular frequency ω. Finally, the steady-state modal amplitudes $X_{\alpha k}(t)$ are related to the generalized displacement $\xi_{\alpha}(r,t)$ of system α in the usual way:

$$\xi_{\alpha}(r,t) = \sum_{k=1}^{n} X_{\alpha k}(t).\ \psi_{\alpha k}(r)$$

with

$$X_{\alpha k}(t) = X_{\alpha k} .\ e^{i\omega t}$$

in the case of pure-tone excitation at ω. Clearly, similar relations hold for system β.

In the case of conservative coupling (i.e. no energy dissipated by the coupling elements) it is easily shown (force from mode $\beta\ell$ to mode αk times velocity of αk equals force from mode αk to mode $\beta\ell$ times velocity of $\beta\ell$) that $\kappa_{\alpha\beta j\ell} = \kappa_{\beta\alpha\ell j}$, $\sigma_{\alpha\beta j\ell} = \sigma_{\beta\alpha\ell j}$ and $\gamma_{\alpha\beta j\ell} = -\gamma_{\beta\alpha\ell j}$. System C1 can now be rewritten

$$M_\alpha\left[(\omega_{\alpha k}^2 - \omega^2) + i\omega\delta_{\alpha k}\right] X_{\alpha k} = F_{\alpha k} - \sum_{j=1}^{m}\left[(\kappa_{kj} - \omega^2\sigma_{kj}) + i\omega\gamma_{kj}\right]X_{\beta j}$$

$$k = 1,2..n$$

[C2]

$$M_\beta\left[(\omega_{\beta\ell}^2 - \omega^2) + i\omega\delta_{\beta\ell}\right]X_{\beta\ell} = F_{\beta\ell} - \sum_{j=1}^{n}\left[(\kappa_{\ell j} - \omega^2\sigma_{\ell j}) + i\omega\gamma_{\ell j}\right]X_{\alpha j}$$

$$\ell = 1,2..m$$

or in a matrix form

$$\begin{bmatrix} \lambda_1 & 0 & \cdots & 0 & \tau_{11} & \cdots & \tau_{1m} \\ 0 & \lambda_2 & \ddots & \vdots & \vdots & & \vdots \\ \vdots & \ddots & \ddots & 0 & \vdots & & \vdots \\ 0 & \cdots & 0 & \lambda_n & \tau_{n1} & \cdots & \tau_{nm} \\ \tau_{11}^* & \cdots & \tau_{1n}^* & & \mu_1 & 0 & \cdots & 0 \\ \vdots & & \vdots & & 0 & \mu_2 & \ddots & \vdots \\ \vdots & & \vdots & & \vdots & \ddots & \ddots & 0 \\ \tau_{m1}^* & \cdots & \tau_{mn}^* & & 0 & \cdots & 0 & \mu_m \end{bmatrix} \begin{bmatrix} X_{\alpha_1} \\ \vdots \\ X_{\alpha n} \\ X_{\beta_1} \\ \vdots \\ X_{\beta m} \end{bmatrix} = \begin{bmatrix} F_{\alpha_1} \\ \vdots \\ F_{\alpha n} \\ F_{\beta_1} \\ \vdots \\ F_{\beta m} \end{bmatrix} \qquad [C3]$$

with

$$\lambda_k = M_\alpha[(\omega_{\alpha k}^2 - \omega^2) + i\omega\,\delta_{\alpha k}]$$

$$\mu_\ell = M_\beta[(\omega_{\beta \ell}^2 - \omega^2) + i\omega\,\delta_{\beta \ell}]$$

$$\tau_{k\ell} = [(\kappa_{k\ell} - \omega^2\,\sigma_{k\ell}) + i\omega\,\gamma_{k\ell}]$$

and where '*' denotes the complex conjugate operator.

It is clear that a general solution of system C3 cannot easily be found. However, as mentioned earlier, two simplified cases can be examined with some hope of success.

First consider the (now well-known) case with two modes (Lyon, 1975). System C3 is reduced to

$$\begin{bmatrix} \lambda_1 & \tau_{11} \\ \tau_{11}^* & \mu_1 \end{bmatrix} \begin{bmatrix} X_{\alpha_1} \\ X_{\beta_1} \end{bmatrix} = \begin{bmatrix} F_{\alpha_1} \\ F_{\beta_1} \end{bmatrix} \quad \text{or} \quad \begin{bmatrix} \lambda & \tau \\ \tau^* & \mu \end{bmatrix} \begin{bmatrix} X_\alpha \\ X_\beta \end{bmatrix} = \begin{bmatrix} F_\alpha \\ F_\beta \end{bmatrix} .$$

Then

$$\Delta = \lambda\mu - |\tau|^2$$

and

$$X_\alpha = \frac{1}{\Delta} \begin{vmatrix} F_\alpha & \tau \\ F_\beta & \mu \end{vmatrix} = \frac{F_\alpha \mu - F_\beta \tau}{\Delta}$$

$$X_\beta = \frac{1}{\Delta} \begin{vmatrix} \lambda & F_\alpha \\ \tau^* & F_\beta \end{vmatrix} = \frac{F_\beta \lambda - F_\alpha \tau^*}{\Delta} .$$

The time averages of energy quantities like the transmitted power, the dissipated power etc. are given by expressions like :-

power transmitted from α to β $= \frac{1}{2}\,\mathrm{Re}\,\{(-\tau^* X_\alpha)(\dot{X}_\beta)^*\}$

$$= \frac{1}{2} \text{Re} \{(-\tau^* X_\alpha)(-i\omega X^*_\beta)\} ,$$

power transmitted from β to α $= \frac{1}{2} \text{Re} \{(-\tau X_\beta)(\dot{X}_\alpha)^*\}$

$$= \frac{1}{2} \text{Re} \{(-\tau X_\beta)(-i\omega X^*_\alpha)\} ,$$

power dissipated by α $= \frac{1}{2} \text{Re} \{(i\omega\delta_\alpha M_\alpha X_\alpha)(\dot{X}_\alpha)^*\}$

$$= \frac{1}{2} \text{Re} \{(i\omega\delta_\alpha M_\alpha X_\alpha)(-i\omega X^*_\alpha)\} .$$

The Statistical Energy Analysis Energy Balance equations are then obtained by integrating these energy quantities (expressed as the real part of complex products) over the frequency variable like

$$\text{power flow (white noise)} = \int_{-\infty}^{+\infty} \text{power flow } (\omega) .\ d\omega \quad .$$

These integrals can theoretically be evaluated from tabulated expressions (Gradshteyn & Ryzhik, 1980, p. 218-219). In this simple case, the computation can actually be carried out analytically (See Lyon, 1975).

Next, consider three modes. System C3 is reduced to

$$\begin{bmatrix} \lambda_1 & \tau_{11} & \tau_{12} \\ \tau^*_{11} & \mu_1 & 0 \\ \tau^*_{21} & 0 & \mu_2 \end{bmatrix} \begin{bmatrix} X_{\alpha_1} \\ X_{\beta_1} \\ X_{\beta_2} \end{bmatrix} = \begin{bmatrix} F_{\alpha_1} \\ F_{\beta_1} \\ F_{\beta_2} \end{bmatrix} .$$

X_{α_1}, X_{β_1} and X_{β_2} can easily be found, but the complex products which correspond to the average energy quantities are extremely cumbersome and the integrals over the frequency variable are formidable. Consequently,

the calculation was abandoned, thus leaving this case unresolved.

Finally, consider the case where all coupling coefficients and modal forces are equal (see above for physical meaning). System C3 now reduces to

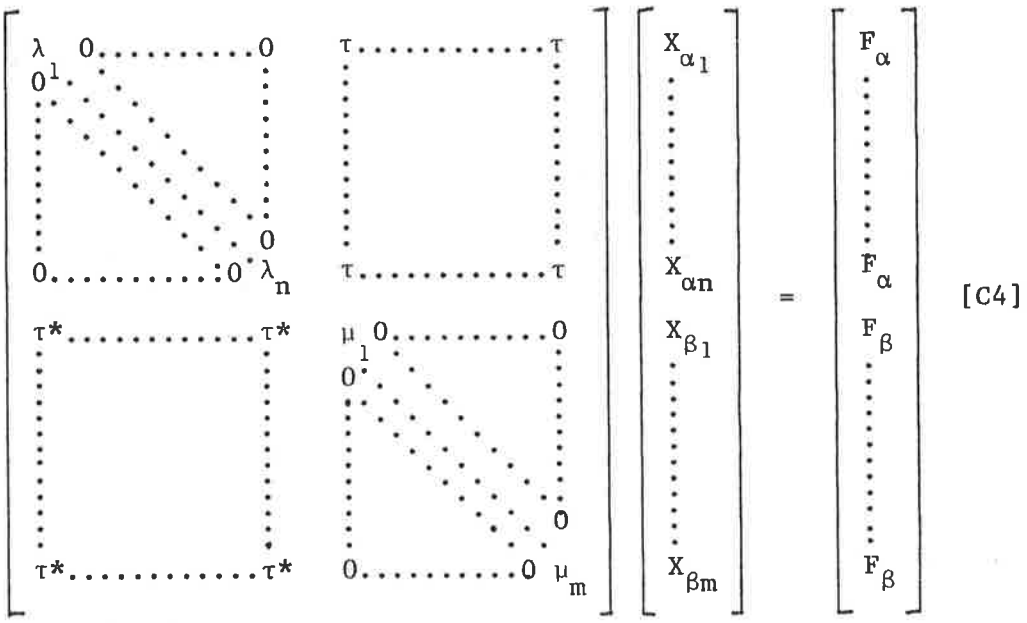

[C4]

This system can be solved analytically as follows. Develop the determinant along the first row :

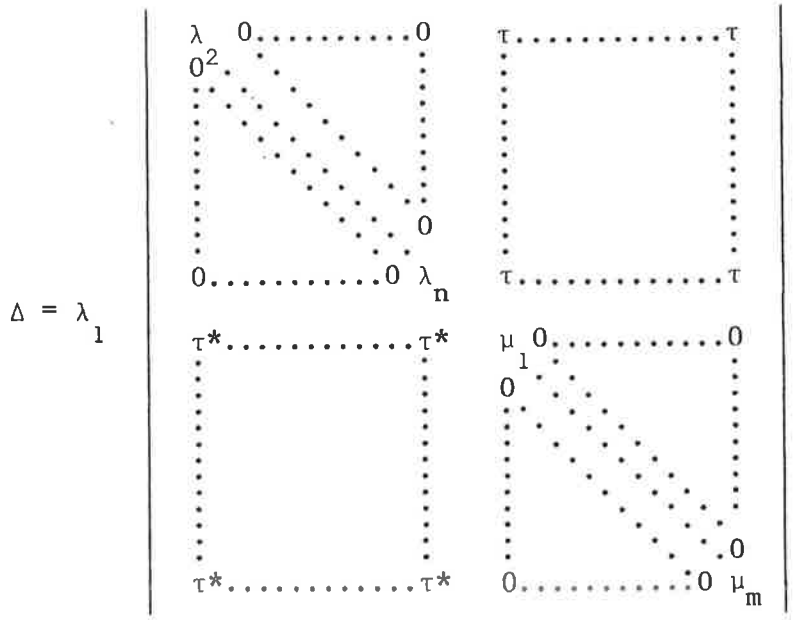

$$+ (-1)^{n}\tau \begin{vmatrix} 0 & \lambda_2 & 0 & \cdots & 0 \\ & \ddots & & & \\ & & & & 0 \\ 0 & \cdots & 0 & & \lambda_n \\ \tau^* & \cdots & \tau^* & & \\ & & & & \\ \tau^* & \cdots & \tau^* & & \end{vmatrix} \begin{matrix} \tau & \cdots & \tau \\ & & \\ & & \\ \tau & \cdots & \tau \\ 0 & \cdots & 0 \\ \mu_2 & 0 & \cdots & 0 \\ 0 & \ddots & & \\ & & & 0 \\ 0 & \cdots & 0 & \mu_m \end{matrix}$$

$$+ (-1)^{n+1}\tau \begin{vmatrix} 0 & \lambda_2 & 0 & \cdots & 0 \\ & \ddots & & & \\ & & & & 0 \\ 0 & \cdots & 0 & & \lambda_n \\ \tau^* & \cdots & \tau^* & & \\ & & & & \\ \tau^* & \cdots & \tau^* & & \end{vmatrix} \begin{matrix} \tau & \cdots & \tau \\ & & \\ & & \\ \tau & \cdots & \tau \\ \mu_1 & 0 & \cdots & 0 \\ 0 & \cdots & & 0 \\ 0 & \mu_3 & 0 & \cdots & 0 \\ & \ddots & & & \\ & & & & 0 \\ 0 & \cdots & 0 & & \mu_m \end{matrix} + \ldots$$

$$\ldots + (-1)^{n+m-1}\tau \begin{vmatrix} 0\ \lambda_2\ 0 \ldots\ldots 0 & \tau \ldots\ldots\ldots \tau \\ \vdots \quad \ddots \quad \vdots & \vdots \qquad\qquad \vdots \\ 0 \ldots\ldots\ldots 0\ \lambda_m & \tau \ldots\ldots\ldots \tau \\ \tau^* \ldots\ldots\ldots \tau^* & \mu_1\ 0 \ldots\ldots 0 \\ \vdots \qquad\qquad \vdots & 0 \quad \ddots \quad \vdots \\ \tau^* \ldots\ldots\ldots \tau^* & 0 \ldots\ldots 0\ \mu_{m-1} \\ & 0 \ldots\ldots\ldots 0 \end{vmatrix}$$

or

$$\Delta = \lambda_1 \Delta^1 + (-1)^n \tau D_1^1 + (-1)^{n+1} \tau D_2^1 + \ldots\ldots + (-1)^{n+m-1} \tau D_m^1 \quad .$$

Δ^1 is similar to Δ and therefore initiates a recursion.

The other m determinants can be written in the same form after appropriate row permutations :

$$D_k^1 = (-1)^{k-1} \begin{vmatrix} 0\ \lambda_2\ 0 \ldots\ldots 0 & \tau \ldots\ldots\ldots \tau \\ \vdots \quad \ddots \quad \vdots & \vdots \qquad\qquad \vdots \\ 0 \ldots\ldots\ldots 0\ \lambda_n & \tau \ldots\ldots\ldots \tau \\ \tau^* \ldots\ldots\ldots \tau^* & 0 \ldots\ldots\ldots 0 \\ \vdots \qquad\qquad \vdots & \mu_1\ 0 \ldots\ldots 0 \\ \tau^* \ldots\ldots\ldots \tau^* & 0 \quad \ddots \quad \vdots \\ & \mu_{k-1} \quad \mu_{k+1}\ 0 \\ & \ddots \quad \ddots \\ & 0 \ldots\ldots 0\ \mu_m \end{vmatrix} \qquad k = 1,2..m \ .$$

Now computation of D_k^1 also initiates a recursion since it can be developed along the first row as

$$D_k^1 = -\lambda_2 \begin{vmatrix} 0 & \lambda_3 & 0 & \cdots & 0 & \tau & \cdots & \tau \\ \vdots & \ddots & \ddots & & \vdots & \vdots & & \vdots \\ & \ddots & \ddots & & 0 & & & \\ 0 & \cdots & 0 & \lambda_n & & \tau & \cdots & \tau \\ \tau^* & \cdots & \tau^* & & & 0 & \cdots & 0 \\ \vdots & & \vdots & & & \mu_1 & \ddots & \vdots \\ & & & & & 0 & \ddots & \\ & & & & & & \mu_{k-1} & \\ & & & & & & \ddots & \mu_{k+1} \\ & & & & & & & 0 \\ \tau^* & \cdots & \tau^* & & & 0 & \cdots & 0 \quad \mu_m \end{vmatrix} + \text{zero terms} = -\lambda_2 D_k^2$$

where the remaining terms are zero by virtue of having two identical rows. Now we have

$$\Delta = \lambda_1 \Delta^1 + (-1)^n \tau (D_1^1 + D_2^1 + \ldots + D_m^1)$$

$$\Delta^1 = \ldots.$$

and

$$D_k^1 = -\lambda_2 D_k^2$$

$$D_k^2 = \ldots. \quad .$$

These recursive formulae produce, after some manipulations, the following result

$$\Delta = (\lambda_1 \lambda_2 \ldots \lambda_n)(\mu_1 \mu_2 \ldots \mu_m)\left[1 - |\tau|^2 \left(\frac{1}{\lambda_1} + \frac{1}{\lambda_2} + \ldots + \frac{1}{\lambda_n}\right)\left(\frac{1}{\mu_1} + \frac{1}{\mu_2} + \ldots + \frac{1}{\mu_m}\right)\right]$$

or

$$\Delta = \pi_{\alpha 0}\pi_{\beta 0} - |\tau|^2 \sum_{k=1}^{n} \pi_{\alpha k} \sum_{\ell=1}^{m} \pi_{\beta \ell}$$

where

$$\pi_{\alpha 0} = \lambda_1 \times \lambda_2 \times \ldots \times \lambda_n$$

$$\pi_{\beta 0} = \mu_1 \times \mu_2 \times \ldots \times \mu_m$$

$$\pi_{\alpha k} = \lambda_1 \times \lambda_1 \times \ldots \times \lambda_{k-1} \times \lambda_{k+1} \times \ldots \times \lambda_n$$

$$\pi_{\beta \ell} = \mu_1 \times \mu_2 \times \ldots \times \mu_{\ell-1} \times \mu_{\ell+1} \times \ldots \times \mu_m \ .$$

Now from system |C4|, X_{α_1} is expressed as

$$X_{\alpha_1} = \frac{1}{\Delta} \begin{vmatrix} F_\alpha & 0 \ldots\ldots 0 & \tau \ldots\ldots \tau \\ & \lambda_2 \ddots & \vdots \\ & 0 \ddots \ddots & \vdots \\ & \ddots \ddots \ddots & \vdots \\ & \ddots \ddots 0 & \vdots \\ F_\alpha & 0 \ldots\ldots 0 \ \lambda & \tau \ldots\ldots \tau \\ F_\beta & \tau^* \ldots\ldots \tau^* \ \mu_1 & 0 \ldots\ldots 0 \\ & \vdots \ddots & \vdots \\ & 0 \ddots \ddots & \vdots \\ & \ddots \ddots \ddots & \vdots \\ & \ddots \ddots 0 & \vdots \\ F_\beta & \tau^* \ldots\ldots \tau^* \ 0 & \ldots\ldots 0 \ \mu_m \end{vmatrix} .$$

Computation of X_{α_1} proceeds in identical fashion to Δ's : develop the determinant along the first row and find two recursive relationships. Finally, one obtains for the steady-state modal responses :

$$X_{\alpha j} = \pi_{\alpha j} \times \frac{F_\alpha \pi_{\beta 0} - F_\beta \tau \sum_{\ell=1}^{m} \pi_{\beta \ell}}{\pi_{\alpha 0} \pi_{\beta 0} - |\tau|^2 \sum_{k=1}^{n} \pi_{\alpha k} \sum_{\ell=1}^{m} \pi_{\beta \ell}} = \pi_{\alpha j} \times \frac{A}{\Delta}$$

$$X_{\beta j} = \pi_{\beta j} \times \frac{F_\beta \pi_{\alpha 0} - F_\alpha \tau^* \sum_{k=1}^{n} \pi_{\alpha k}}{\pi_{\alpha 0}\pi_{\beta 0} - |\tau|^2 \sum_{k=1}^{n} \pi_{\alpha k} \sum_{\ell=1}^{m} \pi_{\beta \ell}} = \pi_{\beta j} \times \frac{B}{\Delta} .$$

These results could be used to compute the complex products which correspond to average energy quantities, and which could be summed over the total number of modes, then integrated over the frequency variable from $-\infty$ to $+\infty$ using tables of integrals (see above).

...ooo000ooo...

BIBLIOGRAPHY

Andersen N., 1974
"On the Calculation of Filter Coefficients for Maximum-Entropy Spectral Analysis". Geophysics, 39(1).

Beranek L.L., 1971
"Noise and Vibration Control". McGraw-Hill.

Bevington P.R., 1969
"Data Reduction and Error Analysis for the Physical Sciences". McGraw-Hill.

Bhattacharya M.C., Mullholland K.A., Crocker M.J., 1971
"Propagation of Sound Energy by Vibration Transmission via Structural Junctions". J. Sound & Vib. 18(2).

Bies D.A., Hamid S., 1980
"In Situ Determination of Loss and Coupling Loss Factors by the Power Injection Method". J. Sound & Vib. 70(2).

Brigham E.O., 1974
"The Fast Fourier Transform". Prentice-Hall.

Brooks J.E., Maidanik G., 1977
"Loss and Coupling Loss Factors of Two Coupled Dynamic Systems". J. Sound & Vib. 55(3).

Burkewitz B., Holmer C., 1980
"Comparison of SEA and Handbook Analysis Procedures for a Noise Propagation Problem". Inter-Noise 1980, Miami, Proceedings.

Chandiramani K.L., 1978
"Some Simple Models Describing the Transition from Weak to Strong Coupling in Statistical Energy Analysis".
J. Acoust. Soc. Am. 63(4).

Crandall S.H., Lotz R., 1971
"On the Coupling Loss Factor in Statistical Energy Analysis".
J. Acoust. Soc. Am. 49(1).

Cremer L., Heckl M., Ungar E.E., 1973
"Stucture-Borne Sound". Springer Verlag.

Crocker M.J., Price A.J., 1969
"Sound Transmission Using Statistical Energy Analysis".
J. Sound & Vib. 9(3).

Davies H.G., 1973
"Random Vibration of Distributed Systems Strongly Coupled at Discrete Points". J. Acoust. Soc. Am. 54(2).

Eichler E., 1965
"Thermal Circuit Approach to Vibrations in Coupled Systems and the Noise Reduction of a Rectangular Box".
J. Acoust. Soc. Am. 37(6).

Fahy F.J., 1970
"Energy Flow Between Oscillators : Special Case of Point Excitation". J. Sound & Vib. 11(4).

Fahy F.J., 1974
"Statistical Energy Analysis - A Critical Review". Shock & Vib. Dig. 6(7).

Gersch W., 1961
"Mean Square Response in Structural Systems". J. Acoust. Soc. Am. 48(1).

Gersch W., 1969
"Average Power and Power Exchange in Oscillators". J. Acoust. Soc. Am. 46(5).

Gradshteyn I.S., Ryzhik I.M., 1980
"Table of Integrals, Series, and Products". Academic Press.

Hamid S., 1981
"The Vibration Response of Built-up Stuctures Modelled as a Collection of Connected Plates". Master's Thesis, Adelaide University.

Harris F.J., 1978
"On the Use of Windows for Harmonic Analysis with the DFT". Proceedings of the IEEE.

Haykin S., 1979
"Nonlinear Methods of Spectral Analysis". Springer Verlag.

Heckl M., 1961
"Wave Propagation in Beam-Plate Systems". J. Acoust. Soc. Am. 33(5).

Heckl M., 1962
"Measurements of Absorption Coefficients on Plates". J. Acoust. Soc. Am. 34(6).

Jensen Ø., 1976
"Calculation of Structureborne Noise Transmission in Ships Using the 'Statistical Energy Analysis' Approach". International Symposium on Shipboard Acoustics.

Kayser K.W., Bogdanoff J.L., 1975
"A New Method for Predicting Response in Complex Linear Systems". J. Sound & Vib. 38(3).

Lotz R., Crandall S.H., 1973
"Prediction and Measurement of the Proportionality Constant in Statistical Energy Analysis of Structures". J. Acoust. Soc. Am. 54(2).

Lyon R.H., 1969
"Statistical Analysis of Power Injection and Response in Stuctures and Rooms". J. Acoust. Soc. Am. 45(3).

Lyon R.H., 1975
"Statistical Energy Analysis of Dynamical Systems : Theory and Application". MIT Press.

Lyon R.H., Eichler E., 1964
"Random Vibrations of Connected Structures".
J. Acoust. Soc. Am. 36(7).

Lyon R.H., Maidanik G., 1962
"Power Flow Between Linearly Coupled Oscillators".
J. Acoust. Soc Am. 34(5).

Lyon R.H., Scharton T.D., 1965
"Vibrational-Energy Transmission in a Three-Element Structure".
J. Acoust. Soc. Am. 38(2).

Maidanik G., 1962
"Response of Ribbed Panels to Reverberant Acoustic Fields".
J. Acoust. Soc. Am. 34(6).

Maidanik G., 1976
"Response of Coupled Dynamic Systems". J. Sound & Vib. 46(4).

Maidanik G., 1976
"Variations in the Boundary Conditions of Coupled Dynamic Systems". J. Sound & Vib. 46(4).

Maidanik G., 1977
"Loss and Coupling Loss Factors of Two Coupled Dynamic Systems". J. Sound & Vib. 55(3).

Maidanik G., 1977
"Some Elements in Statistical Energy Analysis".
J. Sound & Vib. 52(2).

Makhoul J., 1975
"Linear Prediction : a Tutorial Review".
IEEE Proceedings 63(4).

Manning J.E., Remington P.J., 1971
"Statistical Energy Methods". BBN Report No 2064.

Newland D.E., 1966
"Calculation of Power Flow Between Coupled Oscillators".
J. Sound & Vib. 3(3).

Newland D.E., 1968
"Power Flow Between a Class of Coupled Oscillators".
J. Acoust. Soc. Am. 43(3).

Papoulis A., 1977
"Signal Analysis". McGraw-Hill.

Peled A., Bede L., 1976
"Digital Signal Processing". Wiley.

Plunt J., 1980
"SEA - Calculation of Structure-borne Sound in Ship Structures".
Inter-Noise, Miami, Proceedings.

Remington P.J., Manning J.E., 1975
"Comparison of SEA Power Flow Predictions with an 'Exact' Calculation". J. Acoust. Soc. Am. 57(2).

Scharton T.D., Lyon R.H., 1968
"Power Flow and Energy Sharing in Random Vibration".
J. Acoust. Soc. Am. 43(6).

Smith Jr. P.W., 1979
"Statistical Models of Coupled Dynamic Systems and the Transition from Weak to Strong Coupling".
J. Acoust. Soc. Am. 65(3).

Stanley W.D., 1975
"Digital Signal Processing". Reston Pub. Co., Virg.

Stearn S.D., 1975
"Digital Signal Analysis". Hayden Book.

Swift P.B., 1977
"The Vibrational Energy Transmission Through Connected Structures". Ph.D. Thesis, Adelaide University.

Swift P.B., Bies D.A., 1978
"Vibrational Energy Distribution in Coupled Plates".
Conference on Machinery, Vibration and Noise. Adelaide.

Tretter S.A., 1976
"Introduction to Discrete-Time Signal Processing". Wiley.

Ungar E.E., 1967
"Statistical Energy Analysis of Vibrating Systems".
J. of Engineering for Industry. Transactions of the ASME.

Ungar E.E., Koronaios N., 1968
"Vibration Distributions in Multipanel Stuctures : Comparison of Measurements with Statistical Energy Predictions".
Shock & Vib. Bull. 37(2).

Wöhle W., Elmallawany A., 1975
"Generalized Model of the Application of SEA for the Sound Propagation in a Complicated Structure".
J. Sound & Vib. 40(2).

...ooo000ooo...